Fracture Strength
of Silicon Solar Cells

C.P. Chen

October 15, 1979

REA

ACKNOWLEDGMENT

ABSTRACT

In an effort to improve the reliability and lower the cost of solar cells, a test program has been developed to determine the nature and source of the flaw controlling the fracture of silicon solar cells and to provide information regarding the mechanical strength of cells.

This report contains results obtained in the first phase of a test program to develop improved methods for testing the mechanical strength of cells and to evaluate the fracture strength of typical Czochralski silicon solar cells 76 mm (3 in.) in diameter.

Significant changes in fracture strengths were found in seven selected in-process wafer-to-cell products from a manufacturer's production line. The fracture strength data were described by Weibull statistical analysis and can be interpreted in light of the exterior flaw distribution of the samples.

CONTENTS

Figures

Tables

SECTION I

SUMMARY

This report presents the results of an in-house test program at JPL for the Engineering Area of the DOE/JPL Low-cost Solar Array (LSA) Project by the Materials Research and Technology Group, Applied Mechanics Division of the Jet Propulsion Laboratory, California Institute of Technology. The objective of this test program was to evaluate cell cracking characteristics and fracture strength changes in the in-process wafer-to-cell end items taken at different stages of a typical manufacturer's production line. It is anticipated that the information on the nature and source of flaws controlling the fracture of silicon solar cells can lead to enhanced production yields and thus to lower costs.

This effort involved the design, evaluation and assessment of several mechanical strength test methods, and study of their limitations for testing silicon solar cells. A specially designed four-point twisting test was recommended as a standard method for measurement of the mechanical strength of silicon solar cells because of its advantageous characteristics over other conventional methods.

The study was made on typical 3-inch diameter Czochralski silicon wafers and cell samples at seven selected stages in the production cycle of a manufacturer. The test results are summarized in Table 1-1. Significant changes in fracture strength were found as a result of the cell processing steps. The strength of chemically polished wafers increased to more than twice that of as-cut wafers; however, the chemical polishing was not sufficient to reduce the large flaws in the samples, suggesting that more chemical polishing is necessary. A significant increase in the overall strength of wafers from texture etching was evident when texture etched wafers were compared with as-sawn wafers. The strength of completed cells varied with the lot number.

The results of this test program indicate that the strength of silicon wafers and cells is controlled by preexisting exterior (edge and surface) flaws which were generated during wafering or handling. The large critical flaws occurring during a cell process step are carried on to the subsequent processes. The fracture strength data were described by Weibull statistical analysis and can be interpreted in light of the exterior flaw distribution of the samples.

A long tail at the low stress portion of the strength distribution curve was found for several types of samples. The wafers or cells, which in the low strength distribution contain large flaws, are likely to be fractured during subsequent cell processing and handling or in the field service. A proof test would be desirable to eliminate these samples before the subsequent cracking occurs.

Table 1-1. Summary of Test Results

CYLINDRICAL BENDING

Sample Type	Orientation	Strength (MNm^{-2})		Mean Deflection at Failure (mm)
		50% Failure Probability	Range of 90% of Failure	
As-cut Wafer	<100>	134	110-138	1.4
As-cut Wafer	<110>	117	112-132	1.3
Chem. Polished Wafer	<110>	278	132-336	2.8
Chem. Polished Wafer	22.5° off <110>	289	136-363	3.0

BIAXIAL STRENGTH

Sample Type	Strength (MNm^{-2})		Mean Deflection at Failure (mm)
	50% Failure Probability	Range of 90% of Failure	
As-cut wafer	194	165-246	1.3
Chem. Polished Wafer	496	186-841	3.3
Texture Etched Wafer	379	248-455	2.3

Table 1-1. Summary of Test Results (Continued)

FOUR-POINT TWISTING

Sample Type	Strength (MNm^{-2})		Mean Deflection at Failure (mm)
	50% Failure Probability	Range of 90% of Failure	
As-cut Wafer	93	45-103	2.0
Chem. Polished Wafer	217	83-386	4.8
Edge Rounded Wafer	92	58-110	2.5
Texture Etched Wafer Lot B	162	151-186	2.5
Texture Etched Wafer Lot E	176	60-190	3.5
Texture Etched Wafer Lot F	208	144-229	3.6
Mesa Etched and A/R Coated Wafer	214	110-293	3.9
Pre-Ohmic Cell Lot A	172	31-248	2.9
Completed Cell Lot A	152	55-234	3.3
Completed Cell Lot C	207	103-262	3.6
Completed Cell Lot E	214	131-296	3.4

SECTION II

INTRODUCTION

The cracking cell is one of the major sources of solar panel rejection and failure (References 1, 2). Cracking of silicon solar cells during field service and testing is believed to result from the extension of a critical preexisting flaw under stress. Such flaws, probably generated during silicon wafering and cell processing and handling, may therefore control the mechanical strength of silicon solar cells. This information emphasizes the importance of establishing a standard mechanical testing method for evaluating the mechanical strength of silicon solar cells. The data resulting from such testing could be used by manufacturers of solar cells to enhance production yields, improve cell reliability and durability, and ultimately to establish mechanical design criteria that would reduce cell cost and support development of automated production.

A silicon solar cell is an ultrathin disc. Because of various limitations inherent in this unique configuration, standard mechanical testing methods are not readily applicable to stressing a large area of the cell specimen uniformly.

A program for mechanical testing of silicon cells was implemented at JPL in July 1978. The purpose of this report is to present the results obtained from the first phase of this test program, which included the following tasks:

(1) Identification of important factors affecting the strength of silicon solar cells

(2) Determination of a test method to measure cell strength

(3) Design and fabrication of a test jig

(4) Procurement of cell samples

(5) Preliminary test and jig modification

(6) Generation of data regarding typical solar cells

(7) Analysis of test data.

Strength data resulting from studies of brittle materials typically show a great deal of scatter. For this reason the conventional method of representing observed quantities using the arithmetic mean and its standard deviation may not show a meaningful characteristic of strength distribution. A statistical method commonly used to describe the strength of brittle materials is that given by Weibull (References 3, 4). According to this method, a

formula of the form given below is used to relate the probability of failure, G, with stress, S.

$$G = 1 - \exp \left[- \int_V \left(\frac{S - S_u}{S_o} \right)^m dV \right] \qquad (1)$$

where S_u is the stress below which none of the samples will fail, S_o is a normalizing factor, m is termed the Weibull modulus, and V is the volume of material under uniaxial stress where fracture initiates. S_u, S_o and m are material properties and are called Weibull parameters. In Weibull analysis it is assumed that fracture at the most critical flaw under a given stress distribution leads to total failure. Thus, the Weibull method is also called "Weakest Link Statistics".

For material under bending, the critical flaw which causes fracture is mostly on the surface. Thus, the fracture probability, G, for material under bending can be expressed as function of surface area, A:

$$G = 1 - \exp \left[- \int_A \left(\frac{S - S_u}{S_o} \right)^m dA \right] \qquad (2)$$

From this equation it is apparent that the larger the surface area of the material under bending stress, the lower the strength distribution obtained from the test. This phenomenon can be interpreted to mean that the larger the surface area under stress, the greater the probability of finding a larger flaw. Therefore, strength data of brittle material depends on both the test sample size and the test method in which the surface area of the sample is stressed.

The typical Weibull plot to describe strength data of brittle material is shown in Figure 2-1. The strength distribution of this Weibull plot can also be described by the distribution of the critical flaw size in the samples. The larger flaw size is found in the fractured sample at the left-hand side (lower strength) of the curve, while the smaller flaw size is at the right-hand side of the curve.

It is important to note that the Weibull modulus, m, which describes the slope of the curve, is related to the flaw size distribution of a material. The smaller m value indicates greater distribution of flaws, greater scatter of the strength data, and shows a smaller slope on the Weibull curve. The Weibull plot will be used to display and interpret the general characteristics of strength data on silicon solar cells.

A brief assessment of several mechanical strength test methods that are most feasible for testing silicon solar cells is given in Section III of this report, and their limitations are addressed. From
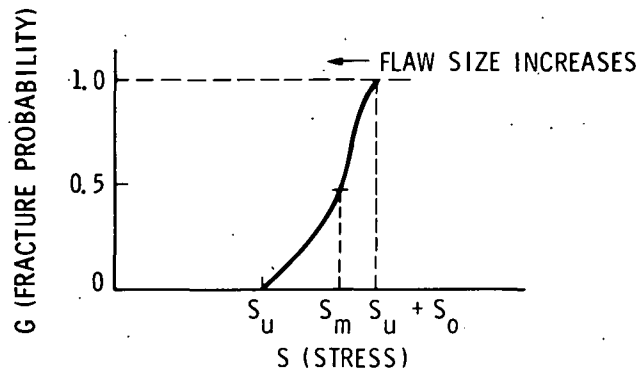
$$\text{FRACTURE PROBABILITY } G = 1 - \exp\left[-\int_V \left(\frac{S - S_u}{S_0}\right)^m dV\right]$$

S_u = STRESS BELOW WHICH NONE WILL FAIL

$S_u + S_0$ = STRESS ABOVE WHICH ALL WILL FAIL

S = STRESS OF INTEREST

m = WEIBULL MODULUS (RELATE TO SLOPE OF PLOT)

S_m = S AT 0.5 G, $S_m \approx S_{ave}$

Figure 2-1. Typical Weibull Distribution (Weakest Link
Statistics) of Strength Data of Brittle Material

this discussion, a standard method for testing solar cell samples is
recommended. Section IV describes the solar cell testing program,
which includes specimen selection, apparatus design and measured
results. A discussion of test results in terms of loading conditions
and the nature of cell processing steps by using Weibull statistical
analysis is presented in Section V. Major conclusions resulting from
the conduct of this test are presented in Section VI. Recommendations
for future work are given in Section VII. Equations for stress
calculation of the test configurations are presented in Appendix A.
Detailed measured cell strength data is given in Appendix B.

2-3

SECTION III

TEST METHOD ASSESSMENT

A.   OBJECTIVE

Conventional methods for testing the strength of ceramic materials are not readily applicable to a thin circular disk like a silicon solar cell because of various limitations inherent in the cell itself. First of all, the thickness to span or width ratio is too small to meet the requirements for conventional test method specimens. Moreover, using conventional methods, stress is concentrated at loading points, producing large deflection, and only a limited portion or none of the cell edge is stressed. Edge flaws are most frequently the origin of fractures in cracked cells. Stress distribution is further complicated by the circular shape of the silicon cell, which imposes additional boundary conditions.

For meaningful interpretation of fracture strength data of silicon solar cells Weibull statistical analysis must be used. Weibull analysis assumes that fracture of brittle material at the most critical flaw under a given stress leads to total failure. The larger the surface area of material under stress, the greater the probability of finding a larger flaw, and the lower the strength distribution that is obtained from the test.

A number of test configurations and loading systems were examined in this study for possible use in determining the strength of silicon solar cells. Detailed analyses were carried out, with emphasis on the following criteria:

(1)   Simple configuration

(2)   Easy to perform

(3)   Easy to adapt in a cell production line

(4)   Self aligning

(5)   Able to stress a large area uniformly.

The "conventional" test methods determined to be most feasible for this purpose were the cylindrical bending test and the biaxial flexure strength test. A specially designed test method referred to as "four-point twisting" had not been evaluated previously but was examined in detail in this study. This test is shown to have desirable features which make it particularly useful for testing the strength of thin disk samples such as silicon solar cells.

B.   ANALYSIS OF TESTS

1.   Cylindrical Bending Test

This method is used conventionally to determine the modulus of rupture (MOR) strength of material for bar or plate samples. The loading method is shown schematically in Figure 3-1. The calculation of MOR strength of material is given in Appendix A.

According to ASTM standards (Reference 5) the thickness to span and width ratio of the specimen for the MOR test should be greater than 1/10 or the following factors should be considered:

(1)   Stress concentration at the loading point

(2)   Large deflection

(3)   Biaxial stress in the center area of the specimen.

The effect of these factors on the measured MOR value were discussed by Giovan (Reference 6). A quantitative evaluation of these factors on the MOR values of silicon solar cells is beyond the scope of present report. However, a strain gage evaluation of a dummy cell under this loading system indicated that the effect of biaxial stress in the center area of a specimen on the MOR value of a solar cell is negligible.

Since the cross-sectional area of the circular specimen under cylindrical bending varies, the stress distribution curve shown in Figure 3-1 deviates from a straight line. In other words, the maximum stress inside is not constant, and the stress distribution would curve concavely downward. The amount of deviation from a straight line depends upon the difference between D and D' in Figure 3-1.

To evaluate the extent of the non-uniformity of stress distribution, a finite element computer analysis of a 3-inch diameter circular disc under cylindrical bending was carried out. The result shows that the maximum stress non-uniformity is less than 10%. Therefore, under the cylindrical bending test the stress distribution of a silicon solar cell can be assumed to be constant, as shown in Figure 3-1, and the MOR value can be estimated by Equation A-2 of Appendix A.

Since the bending stress at the extreme fibers of the sample under cylindrical bending is uniaxial, this test would be useful to determine the uniaxial tensile strength of silicon wafers at different crystalline orientations. The effect of crystalline orientation on the MOR strength of silicon wafers will be discussed later.

One drawback of this test is that only portions of the sample and edges of the sample are stressed. Due to the stress concentration under the loading points, the inner span of the test fixture must be designed in such a way that less than 25% of the wafer edge is tested. This limitation has made this test less desirable for evaluation of the mechanical strength of silicon solar cells.
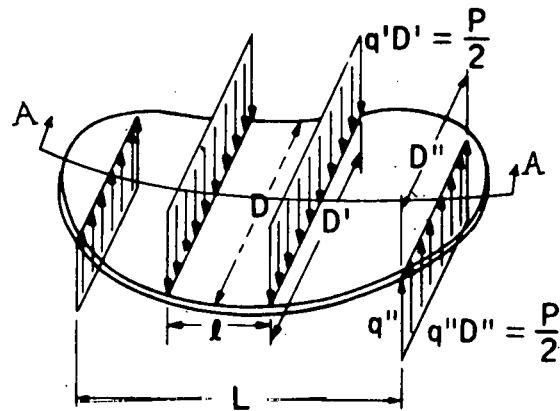
SCHEMATIC
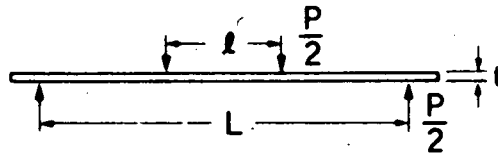
SIDE VIEW OF A-A SECTION
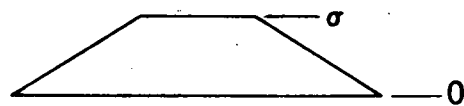
STRESS DISTRIBUTION OF A-A
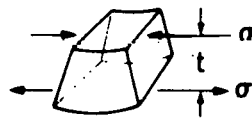
UNIT WIDTH ELEMENT WITHIN ℓ AREA

Figure 3-1. Cylindrical Bending of a Solar Cell

2.   Biaxial Flexure Strength Test

This test method is used to evaluate the effect of biaxial
stress on the strength of a silicon cell. It is described in ASTM
F394-74T (Reference 7) for the determination of biaxial flexure
strength of thin ceramic substrates. The loading method is shown
schematically in Figure 3-2. The stress calculation is given in
Appendix A.

This test method has been studied rather extensively on glass
(Reference 8) and ceramics (References 6, 9). The details of stress
distributions were described (Reference 10). The conditions of use of
this test are given as follows (see Figure 3-2):

   (1)   The thickness of the plate should not be greater than 1/5
          of the diameter of the support ($t \leq 0.4$ a).

   (2)   The maximum deflection (δ_f) should be less than half the
          thickness ($\delta_f \leq 0.5$ t).

   (3)   The radius of the center loading plunger should be greater
          than or equal to 1.7 times of the thickness ($b \geq 1.7$ t)

In order to determine the strength of silicon solar cells, the
test method should be able to stress sample areas as large as
possible. Since the thickness (t) of the solar cell is so small, the
use of the biaxial strength test for solar cells cannot meet condition
2 and can cause stress concentration at the center loading ring. In
addition, the maximum stressed surface area in this test is confined
within the central region of the specimen; fracture is not dependent
upon the condition of the specimen's edge which has been found to be
the major source of cell cracking.

Despite these disadvantages and limitations, this test method is
simple and symmetrical, and appears to be useful to determine the
relative intrinsic strength of the solar cell. Above all, data
regarding the biaxial strength of silicon is of interest and
importance for engineering purposes.

In order to minimize stress concentration, the biaxial strength
test jig should be designed in such a manner that the central
equibiaxial stress area is small, e.g., limited to 12.7 mm (0.5 in.)
in diameter. Therefore, a very small central region (~10% of total
area) was tested by this test. The biaxial stress can be calculated
by Equation A-3 in Appendix A. The stress distribution was verified
by the strain gage measurement.

3.   Four-Point Twisting Test

This method is used to evaluate the twist (shear) strength of a
silicon cell. The cell sample is loaded by four equal vertical forces
that are equally spaced at the edge: two diagonally opposite forces
acting upwards and the other two acting downwards, as shown
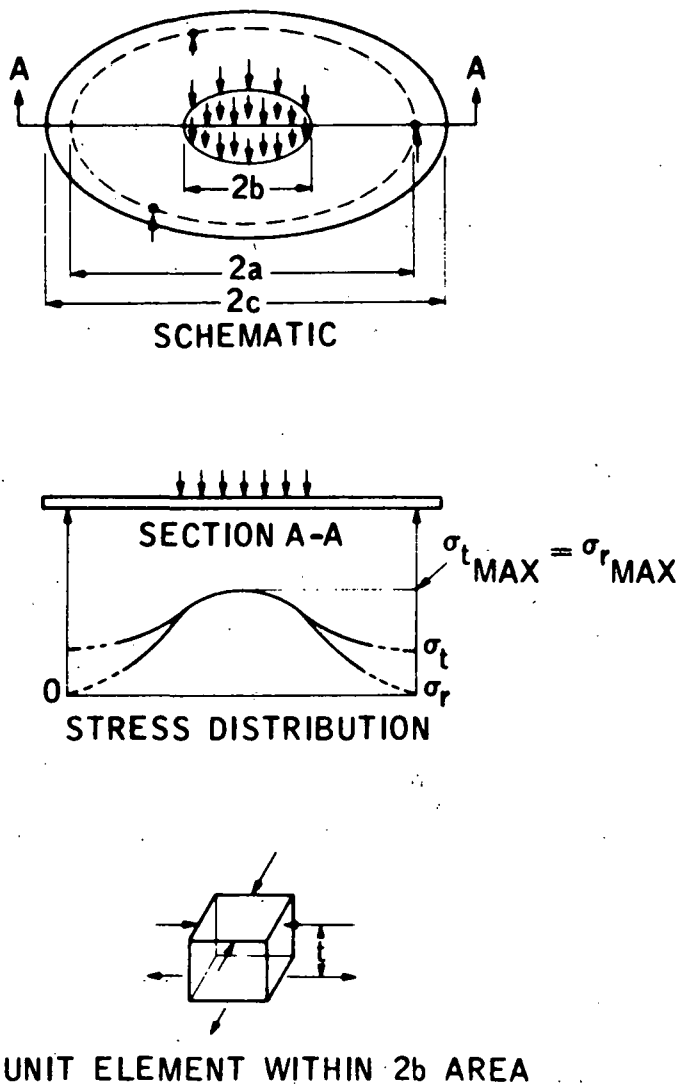
Figure 3-2. Biaxial Strength Test of a Solar Cell

schematically in Figure 3-3. The shear stress calculation is given in Appendix A.

A finite element computer analysis of a 76 mm (3 in.) diameter elastic disc subjected to four-point twisting was carried out; a stress concentration was found at the area of loading points. This problem may make the stress distribution complicated in this area. However, in the area away from the loading points, a uniform shear stress is found in the direction 45° from the axes of two pairs of loading (Figure 3-3). This stress distribution has been verified essentially by strain gage examination.

A stress analysis of a rectangular cross section member subjected to a torsion, T, was made (Reference 11). The maximum twist

stress τ_s for a circular disc under four-point twisting is derived in Appendix A and can be estimated by Equation A-6.

$$\tau_s = \frac{3P}{2t^2}$$

where t is the thickness of the wafer

P is the total fracture force

SCHEMATIC

SECTION A-A

ELEMENT B
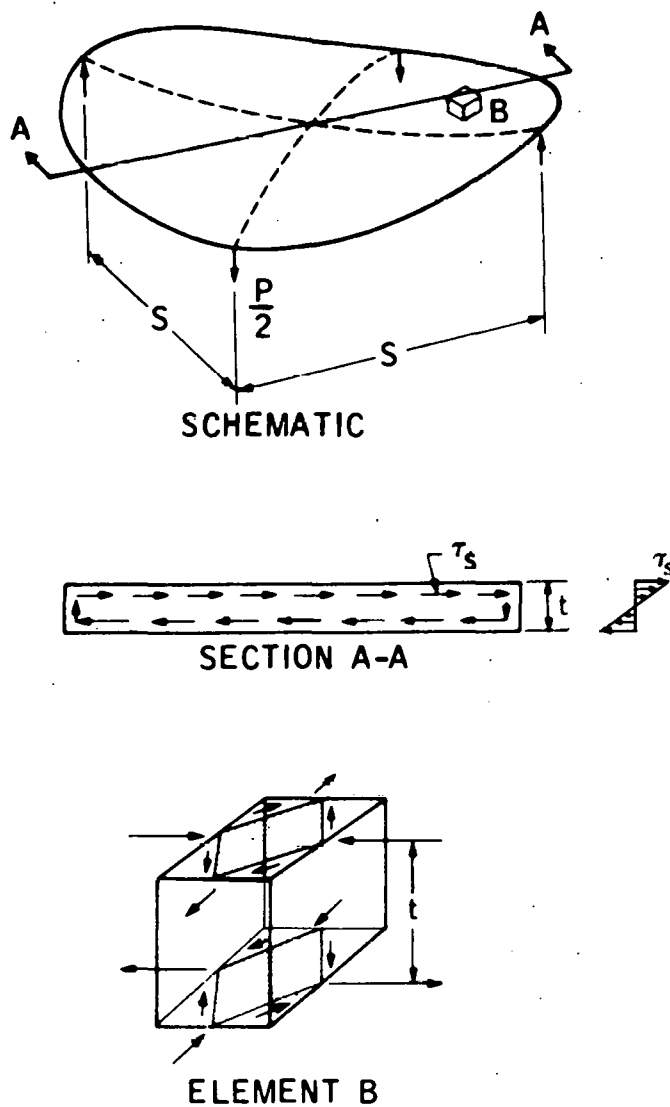
Figure 3-3. Four-point Testing of a Solar Cell

The expected limitations of this test method, such as stress concentrations and large deflection, are beyond the scope of the present report and have not been examined. It is recommended that these areas be investigated in more detail analytically and experimentally.

The four-point twisting test has a simple loading configuration, self alignment, is symmetrical, easy to perform, and stresses the entire wafer specimen, including the edge and internal areas.

C.   CONCLUSIONS

The limitations that are common to all three test methods, i.e., stress concentrations at the load point and large deflection, appear to be due to the form of the solar cell sample itself. These limitations can be minimized by proper test jig design, such as use of a teflon washer at the loading point.

Cylindrical bending proved to be useful to determine the uniaxial tensile (MOR) strength of silicon wafers at different crystalline orientations. One drawback is that less than 25% of the sample and the sample edges are tested.

The biaxial strength test is simple and symmetrical, and appears to be useful to determine the relative strength of the solar cell. However, this method tests a very small central region of the sample; edges of the sample are not stressed. Edge flaws have been found to be the major source of cell cracking, controlling the fracture strength.

The four-point twisting test not only has a simple and symmetrical loading configuration, but also has self-alignment and is easy to perform. In addition, it stresses the entire wafer specimen, including edges and internal area. Four-point twisting is therefore recommended as a standard method for testing the mechanical strength of silicon solar cells.

SECTION IV

SOLAR CELL TESTING

A. OBJECTIVE

To evaluate cell cracking characteristics and changes in fracture strength of silicon solar cells in a typical production line, a representative manufacturer with processing facilities for the complete end-to-end production of typical 76 mm (3 in.) diameter Czochralski solar cells was identified, and samples were procured and studied at several key cell production process steps. A loading fixture was designed and fabricated to perform mechanical strength tests. The test specimens, test apparatus and test results are described in the following pages.

B. SPECIMEN

Typical solar cells produced by several manufacturers were considered for use in this test effort. Those selected for study were the products of a specific manufacturer* with processing facilities for the complete end-to-end production of solar cells. Starting from silane and continuing through polycrystalline silicon to single crystal ingots and sawing of wafers, all of the process steps required to make the completed cell are included. In addition, this manufacturer indicated willingness to provide test samples.

The test specimens included a series of wafer and cell samples 76 mm (3 in.) in diameter taken at several process steps** as follows:

(1) As cut wafers (multi-wire slurry wafering)

(2) Chemically polished wafers***

(3) Edge rounded wafers

(4) Texture etched wafers

(5) Mesa etched and anti-reflection (A/R) coated wafers

(6) Pre-ohmic cells

(7) Completed (metallized) cells

---

* Motorola Inc., Semiconductor Division, Phoenix, AZ.

** Processing procedures are proprietary information.

***Chemical polishing is not used in the regular cell processing. These wafer specimens were made from as-cut wafers (no edge rounding) for the strength evaluation only. All other wafers and cells of the subsequent processes were made from edge rounded wafers.

The properties of the silicon material are given as follows: <100> orientation; boron doped, P-type; resistivity ranging from 0.8 to 2.0 ohm-cm.

C.   TEST APPARATUS

A test fixture was designed so that it could perform cylindrical bending tests, three-point support biaxial flexure strength determinations and four-point twisting tests of silicon solar cell by simply rearranging, removing, or adding dowel pins (8 mm in diameter) and components. The fixture arrangement for each test is described below.

1.   Cylindrical Bending

The cylindrical bending test fixture for solar cells is shown in Figure 4-1. Two lower blocks provide line supports for the cell specimen. Each supporting block is guided into position by three dowel pins and can be pivoted at the middle pin. The upper loading piece was fabricated to be pivoted at a ball bearing at the center. Vinyl electrical tape* was applied on the loading lines of the test fixture to minimize the possibility of stress concentration. The inner span (ℓ) and outer span (L) (see Figure 3-1) are 25.4 mm (1.0 in.) and 55 mm (2.165 in.), respectively.

2.   Biaxial Flexure Strength

The biaxial flexure strength test jig for solar cells is shown in Figure 4-2. The specimen is supported by three dowel pins equally spaced in a circle 63.5 mm in diameter. A teflon washer (12.7 mm o.d., 1.7 mm thick) was applied at each contact point of the dowel pin to minimize the stress concentration. The center loading area is also 12.7 mm (0.5 in.) in diameter, the size of the teflon washer at the contact point of the dowel pin. This test fixture was designed for cells 76 mm (3.0 in.) in diameter, which is a typical size for most solar cells currently manufactured. Therefore (see Figure 3-2), 2a = 63.5 mm (2.5 in.), 2b = 12.7 mm (0.5 in.), and 2c = 76.2 mm (3.0 in.).

3.   Four-Point Twisting

The four-point twist jig for solar cells is shown in Figure 4-3. During the test, two dowel pins on the bottom disk act upwards while the other two, which are 90° apart on the upper disk act downwards to give a shear stress at 45° in the cell specimen, as shown in Figure 3-3. A teflon washer (12.7 mm o.d., 1.7 mm thick) was used at the contact point of each dowel pin. These four dowel pins were designed in a 63.5 mm (2.5 in.) diameter circle.

---

*Scotch Brand, 33+, 20 mm wide x 0.18 mm thick.
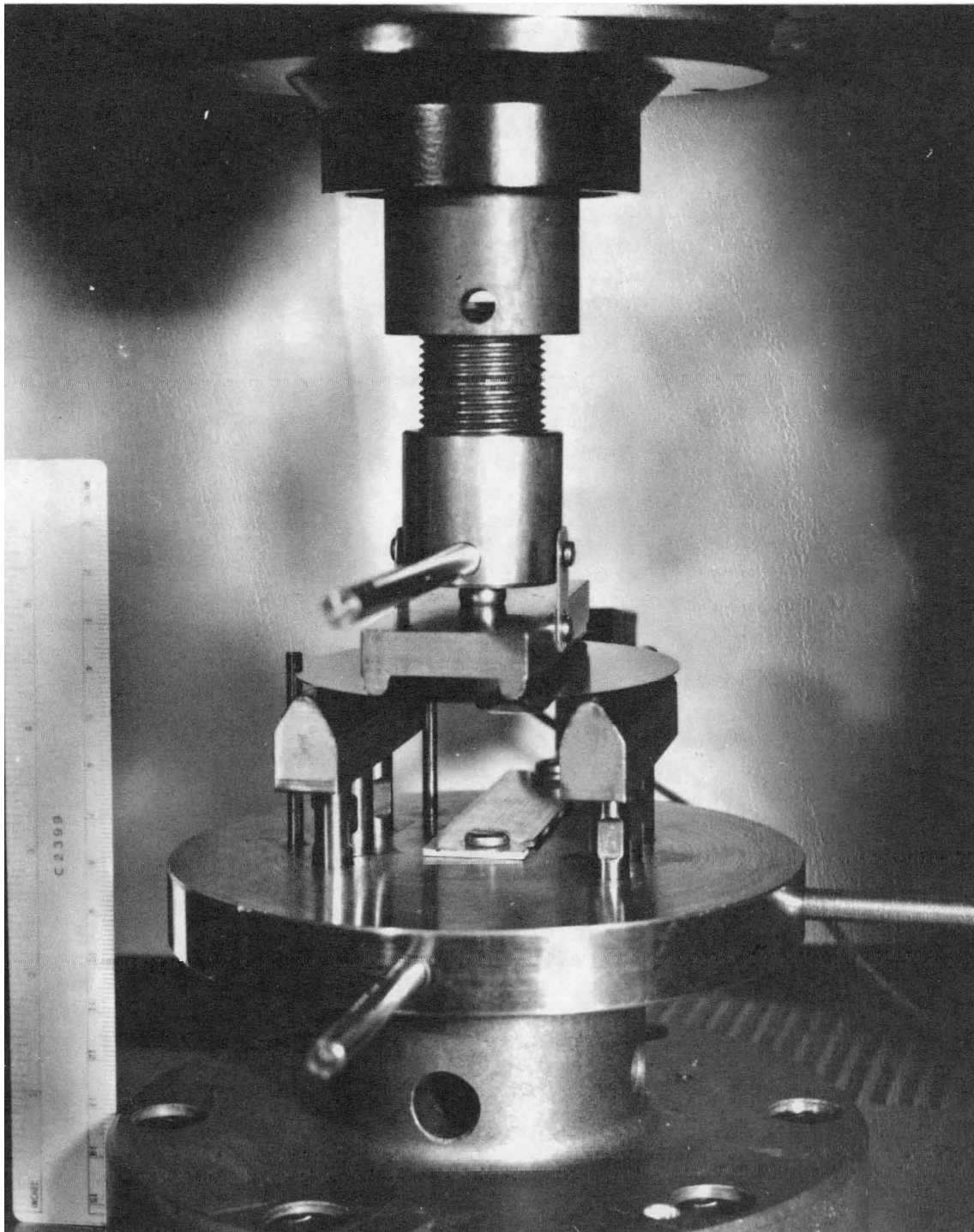
Figure 4-1. Solar Cell Cylindrical Bending Jig
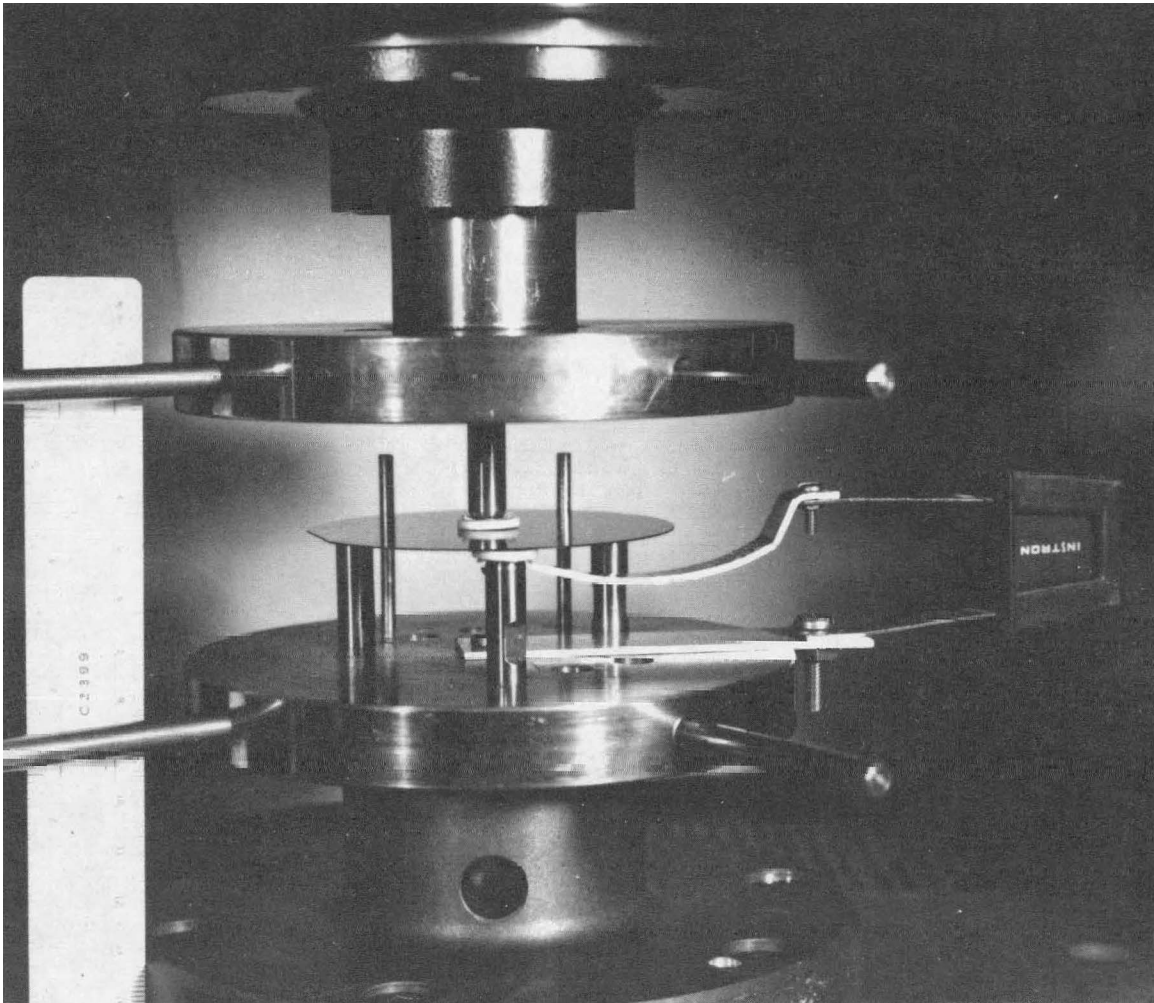
Figure 4-2. Solar Cell Biaxial Flexure Strength Test Jig
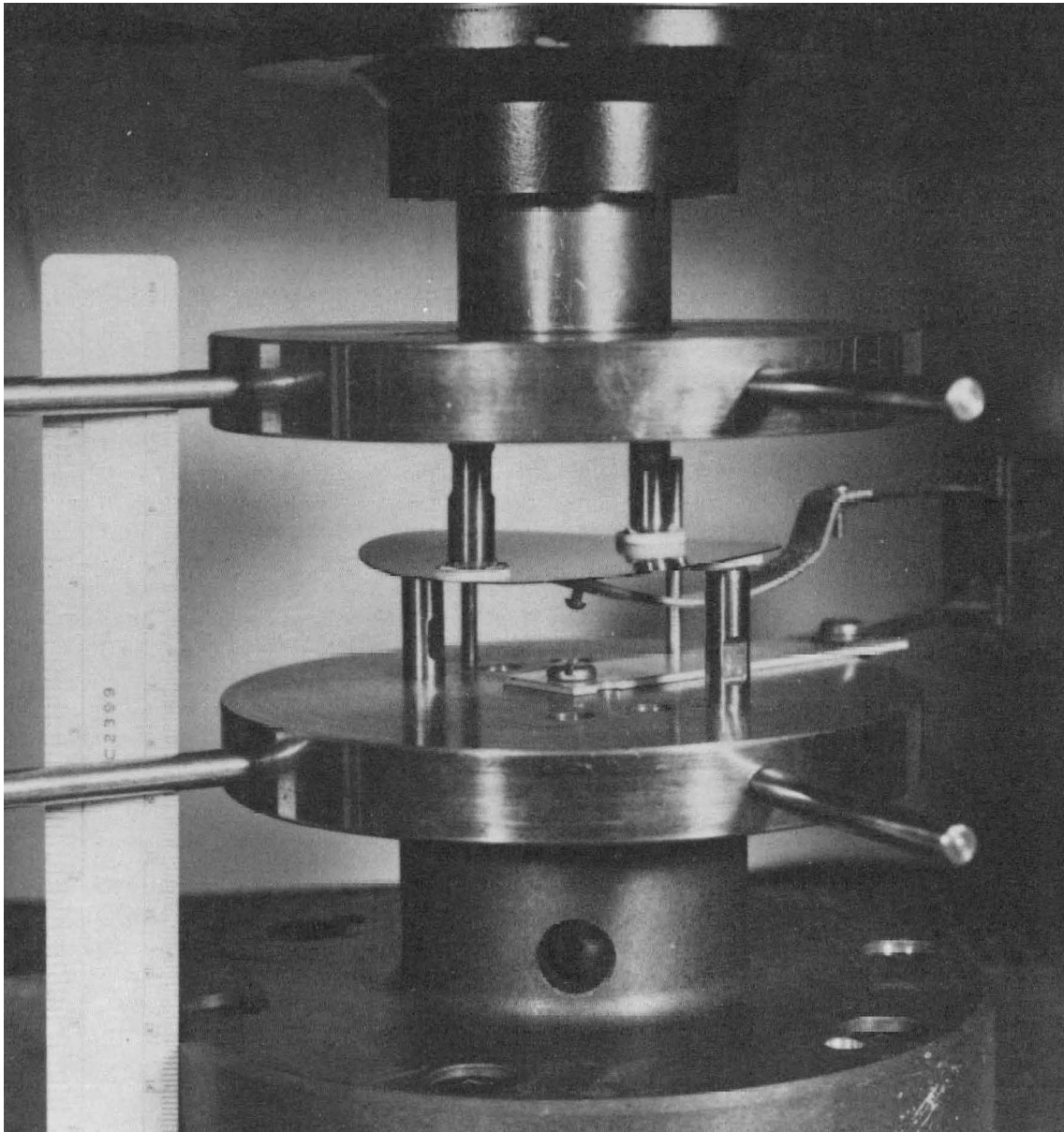
Figure 4-3.   Solar Cell Four-point Twist Jig

D.   TEST IMPLEMENTATION

Prior to each test the thickness of each specimen was measured
at five positions, as shown in Figure 4-4, in order to determine the
thickness variation of the specimen. The maximum thickness variation
of wafers was approximately 0.013 mm (~ 0.0005 in.) and that of
completed cells was up to 0.05 mm (~ 0.002 in.) because of nonuniform
solder. However, the thickness used for the fracture stress
calculation was as follows:

     (1)   Cylindrical bending test - the minimum thickness in the
            test orientation.

     (2)   Biaxial flexure strength - the thickness at the center.

     (3)   Four-point twisting - the minimum thickness at the edge of
            the specimen.

For specimens undergoing cylindrical bending and biaxial strength
tests, scotch tape was applied on the compressive surface of the test
specimen to retain segments after fracture. Tape was not used on
specimens subjected to 4-point twisting, since shear stress existed on
both surfaces.

The deflection of each cell during testing was monitored by an
extensometer* and recorded on an x-y plotter.** The load was applied
by an Instron Testing Machine*** with loading rate 0.1 in./min and
chart speed 2 in./min. Detailed results for each test are given in
Appendix B in Tables B-1 to B-18.

To make meaningful correlation of these data, the measured
strengths for each test sequence were presented in a Weibull plot
describing probability of failure as a function of strength. The
caracteristics of these plots are illustrated and discussed in the
following section.

---

* Strain Gage Extensometer, G51-12A, range: 0-0.500 in., Instron
  Corporation, Canton, MA.

** X-Y Recorder, Model 135A, F. L. Moseley Co., Pasadena, CA.

***Instron Corporation, Model 1122, Canton, MA.
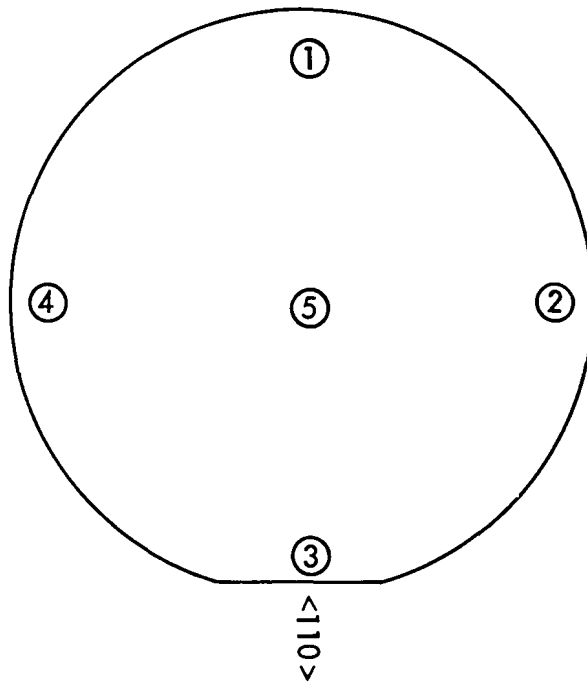
Figure 4-4. Locations of Specimen Cell Thickness Measurement

DISCUSSION OF TEST RESULTS

A. EFFECT OF TEST METHODS ON STRENGTH DATA OF SILICON WAFERS

As-cut and chemically polished wafers under four-point twisting, uniaxial MOR and biaxial strength were used to evaluate the effect of test methods on the strength of wafers. Weibull plots of these strength data are shown in Figure 5-1. In this figure, the strengths of as-cut wafers at 50% failure probability under twist, MOR, and biaxial stresses are approximately 93, 117, and 194 MNm^{-3} (14, 17, and 28) ksi), respectively. Similarly, the strengths of chemically polished wafers at 50% failure probability are 217, 278, and 496 MNm^{-2} (31, 40, and 72 ksi) for twist, MOR, and biaxial stresses, respectively. As mentioned before, the larger the surface area of the sample under stress, the greater the probability that the largest flaw will be under stress. The four-point twisting test can stress almost the entire wafer area; cylindrical bending to determine the MOR strength can stress less than 30% of the wafer surface and edge, while the biaxial strength test stresses only 10% of the surface area at the center and none of the specimen's edge. Therefore, the measured strength under biaxial stress is much higher than that under cylindrical bending or twisting. The twist strength of as-cut wafers is the lowest among these three methods.
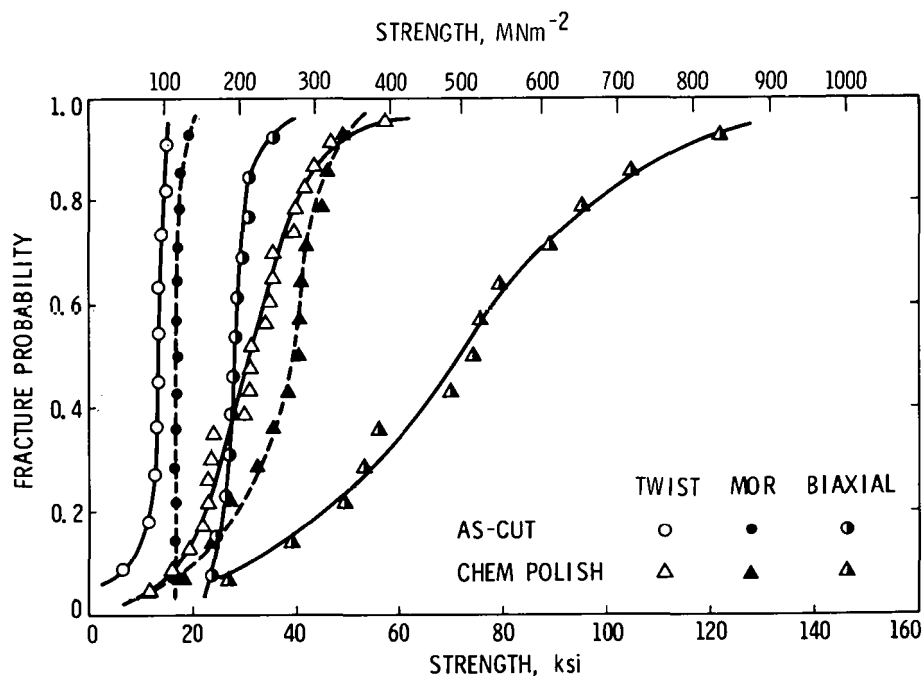
Figure 5-1. Effect of Test Methods on the Measured Strength of Silicon Wafers

B.   EFFECT OF CRYSTALLINE ORIENTATION ON THE MOR OF SILICON WAFERS

As-cut and chemically polished wafers under cylindrical bending are used to evaluate the effect of crystalline orientation on the strength of silicon wafers. Cylindrical bending was used here as it is highly directional in its stress application. Weibull plots for as-cut wafers tested in <100> and <110> orientations are shown in Figure 5-2. The plots for chemically polished wafers in <110> and 22.5° off <110> (half way between <100> and <110>), respectively, are also shown in Figure 5-2. It can be seen that the Weibull distributions of MOR for as-cut wafers in <100> and <110> orientations are very close. A similar relationship exists between the Weibull distributions for chemically polished wafers in <110> and 22.5° off <110>. Therefore, the effect of crystalline orientation on the strength of silicon solar cell does not appear to be significant.

The typical fracture modes of silicon wafers subjected to cylindrical bending is shown in Figure 5-3. The fracture of wafers under <110> bending is found to be in {111} planes at <110> direction; under <100> bending cracking is found in {111} planes in <110> orientations and ziz-zags in the <100> loading direction. These fracture modes and lack of sensitivity to crystallographic orientation suggest that the strength of silicon wafers is controlled by crack initiation but not crack propagation. The fracture origin of tested cells was examined and found to be edge flaws. The quantitative measurement of the critical flaw size of each sample is beyond the scope of the present report.
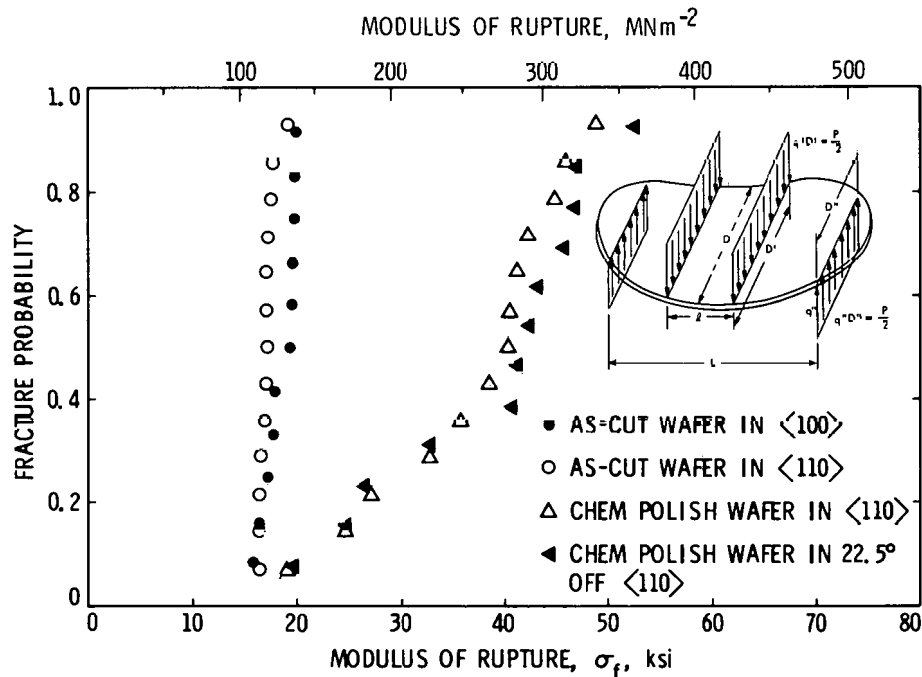
Figure 5-2.   Effect of Crystalline Orientations on Modulus of Rupture Strength of As-cut and Chemically Polished Silicon Wafers

⟨110⟩   ⟨100⟩
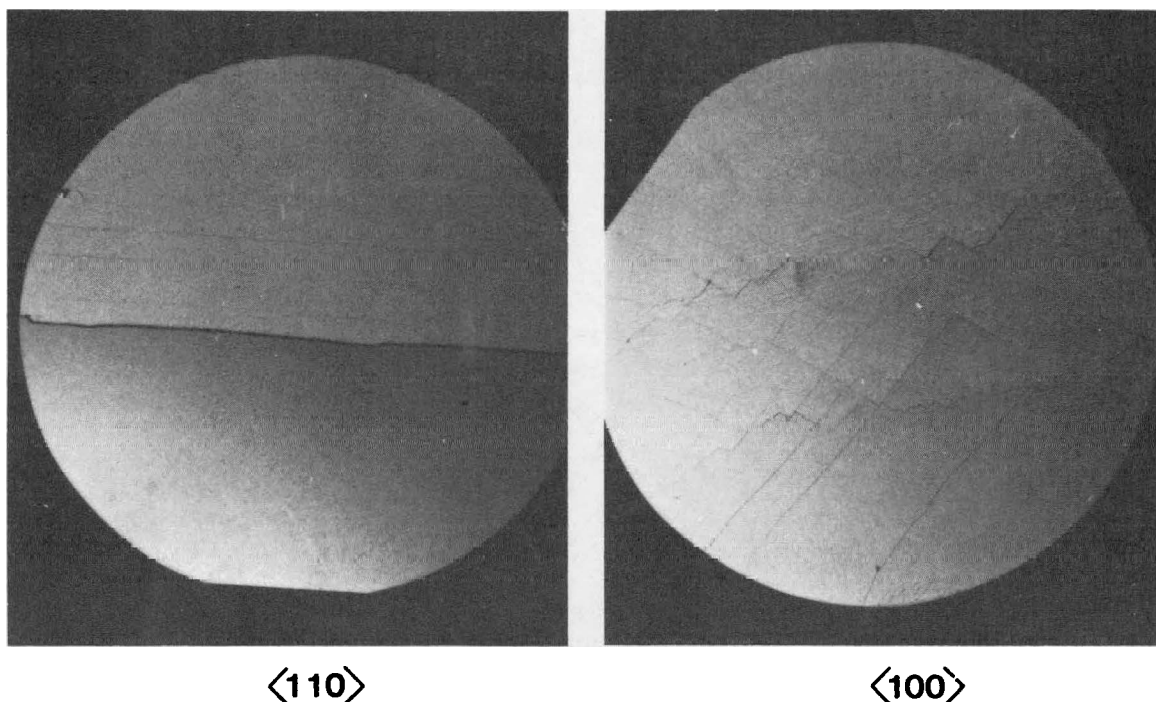
Figure 5-3. Fracture Modes of As-cut Wafers

The MOR value for chemically polished wafers at 50% fracture probability is approximately 278 MNm^{-2} (40 ksi), which is more than twice the strength of as-cut wafers. Chemical polishing is shown to be effective in reducing surface flaws of wafers resulting from wafering. This subject will be discussed later.

C.   BIAXIAL STRENGTH OF SILICON WAFERS

The biaxial strength distributions of as-cut, chemically polished, and texture etched wafers are plotted in Figure 5-4. The biaxial strength at 50% fracture probability for as-cut wafers is 194 MNm^{-2} (28 ksi) and that for chemically polished wafers is 496 MNm^{-2} (72 ksi). A greater than twofold increase in strength results from chemical polishing, and a similar increase is seen for texture etching.

As can be seen in Figure 5-4, chemical polishing is more effective for reduction of the smaller surface flaws than of the larger flaws, such that a greater increase in strength is found at higher strengths than at the lower strength portion of the distribution curve. The thickness of chemically polished wafers was approximately 50 μm (~0.002 in.) smaller than that of as-cut wafers, suggesting that more extensive chemical polishing is necessary.
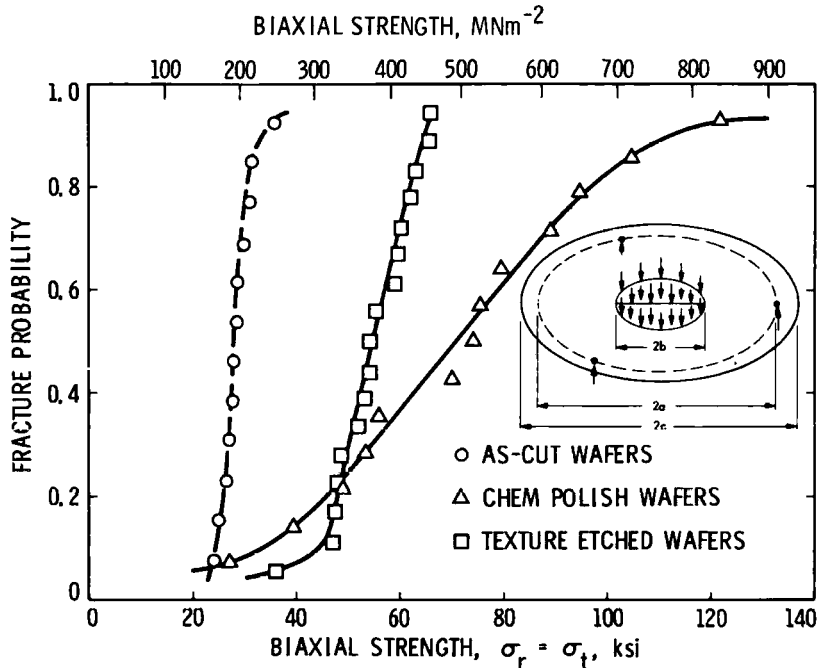
Figure 5-4. Biaxial Strength of Silicon Wafers

Texture etched wafers were produced by chemical etching from as-cut (with edge rounded) wafers. In this process, a dense population of tiny pyramids covering the entire surface of each cell was generated by chemical etching at the preferential crystalline direction. This pyramid-textured surface has been demonstrated to intercept the reflected sunlight and to increase cell performance.

The overall strength of texture etched wafers is greater than that of as-cut wafers (Figure 5-4) as a result of surface flaw reduction by etching. Although the mean strength of texture etched wafers is lower than that of chemically polished wafers, it should be pointed out that the strength of the wafers at low fracture probabilities is the region of interest. The texture teching has the effect of reducing large flaws and providing a more uniform distribution of small flaws associated with the roots of the pyramids. This leads to a more uniform breakage strength than does chemical polishing. Increased chemical polishing may, however, also improve this low-fracture probability region.

It should be noted that the strength of specimens under the biaxial stress test is controlled by the surface area confined within a small central region, whereas under cylindrical bending less than 30% of the total edge and surface area of the specimen is tested. Therefore, the surface condition of the specimen is important for biaxial strength measurement. Angle lapping was used to determine the surface damage from these types of wafers. Microphotos of the angle lapped areas of typicl as-cut, chemically polished, and texture etched wafers are shown in Figure 5-5. The average depth of surface damage is estimated to be 55, 35, and 40 μm for as-cut, chemically polished,
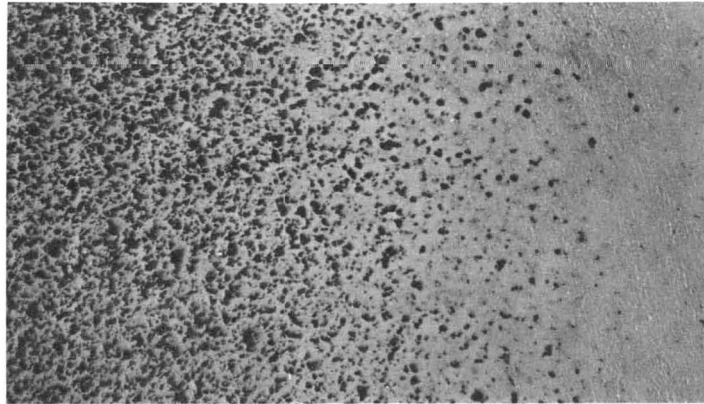
As-cut Wafer
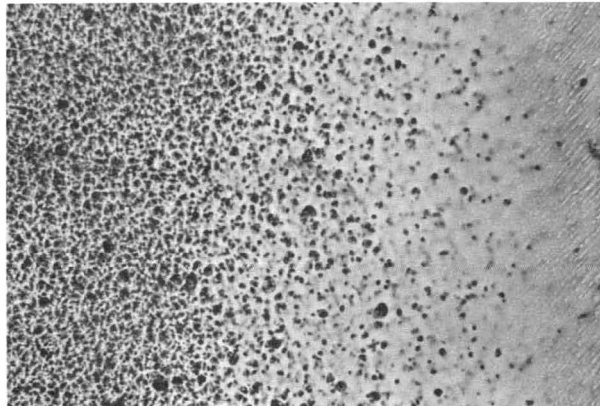
Chemically Polished Wafer
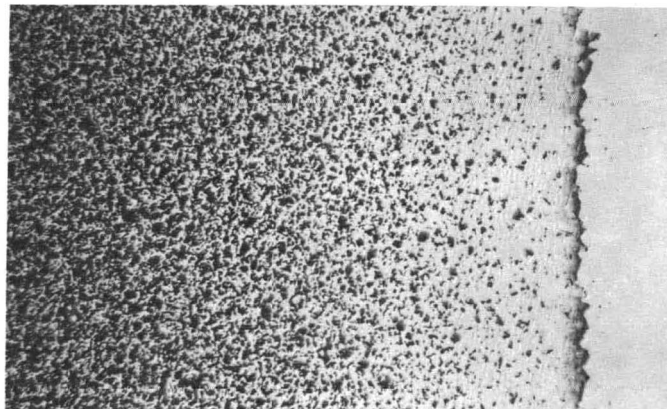
Texture Etched Wafer

Figure 5-5. Typical Angle Lapped Surface Areas for As-cut,
Chemically Polished, and Texture Etched Wafers
(Lapping angle is 2° 52')

and texture etched wafers, respectively. The average depth of surface damage correlates with the mean strength of these wafers.

The typical fracture modes of as-cut and chemically polished wafers subjected to the biaxial flexture test are shown in Figure 5-6. The fracture of silicon wafers was found to be initiated at the center of the specimen where the maximum biaxial stress occurred under this test configuration. Much finer segments resulted from the fracture of chemically polished samples than from as-cut samples. The measured strength of chemically polished wafers is greater than that of as-cut samples; thus more energy is available to initiate a larger number of cracks simultaneously.

D.   EFFECT OF CELL PROCESSES ON THE TWIST STRENGTH OF WAFERS

As discussed in Section III C, the four-point twisting test was recommended to be a standard method for testing the mechanical strength of silicon solar cells. The twist strengths of silicon wafers at several cell process steps are shown in Figure 5-7. Figure 5-8 compares the strength of the completed (metallized) cell with that of the end items of several preceding process steps. The following observations have emerged from twist strength data recorded at various process steps in the production of silicon cells:

1.   The twist strengths of both as-cut and edge rounded wafers at 50% fracture probability are the same: 93 MNm^{-2} (13.5 ksi). The Weibull distributions for these two types of wafers are also

Chemically Polished   As-cut
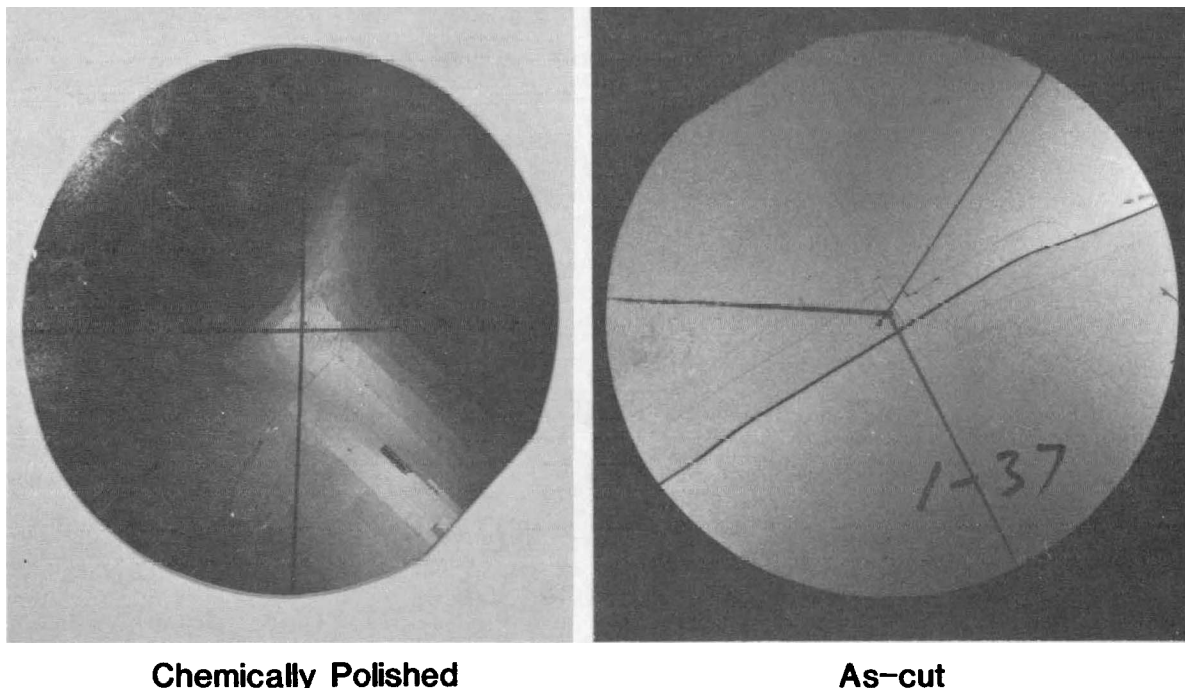
Figure 5-6.   Typical Fracture Modes of As-cut and Chemically
               Polished Wafers Subjected to Biaxial Flexure Test
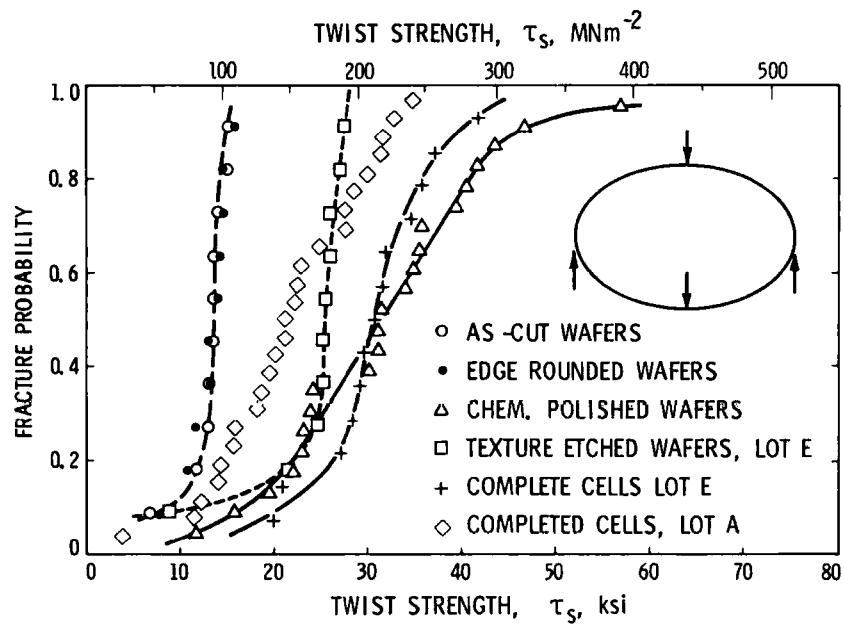
Figure 5-7. Effect of Cell Processes on the Twist Strength
of Silicon Wafers and Cells
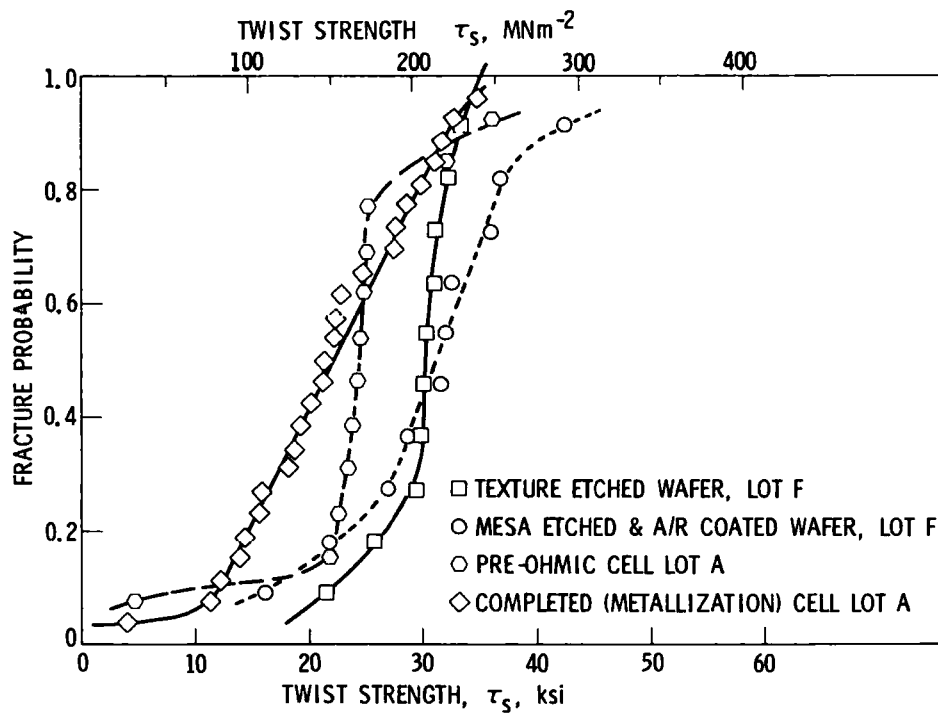
Figure 5-8. Effect of Metallization and Other Cell Processes
on the Strength of Solar Cells

5-7

identical. The mechanical edge rounding method produces no increase in the strength of silicon wafers. The manufacturer has reported that edge rounding has been used to reduce cell cracking from edge corner damage occurring during cell processing and handling. An improved edge-rounding method that can remove edge corners and flaws and increase the strength of silicon wafers needs to be developed.

2. The twist strength of chemically polished wafers at 50% fracture probability is 217 MNm^{-2} (31.5 ksi), which is more than twice the strength of as-cut wafers. Similar results were obtained from the cylindrical bending and biaxial strength tests (Figures 5-2 and 5-4, respectively). A reduction of flaw size must occur during the chemical etching process, since the strength of wafers is controlled by the critical flaw size. Chemical polishing appears to be more effective in reducing smaller flaws than larger flaws; the slope of the Weibull plot for the strength of chemically polished wafers is smaller than that for as-cut wafers. This implies that more etching on the wafer edge may be necessary to further eliminate the large flaws and improve the strength of silicon wafers.

3. The twist strength of texture etched wafers lot E at 50% fracture probability is 176 MNm^{-2} (25.5 ksi), which is higher than that of as-cut wafers. This suggests that texture etching is effective in improving the strength of wafers. As discussed before, texture etching reduces the surface damage from ingot cutting. It is of importance to note that a tail below 20% fracture probability on the strength distribution curve is usually found in each strength measurement of wafers. As seen in Figure 5-7, an appreciable long tail in the minimum strength end of the curve is found for this lot of texture etched wafers. Texture etched wafers that fail below the 20% fracture probability curve are particularly vulnerable to fracture during subsequent cell processing and handling. Proof testing is useful for truncating the strength distribution of ceramics (Reference 12). A proof test at a proper stress level can be implemented atter texture etching to reduce cell fracture during subsequent cell processes.

4. The twist strength of completed cells (lot E) at 50% fracture probability is 214 MNm^{-2} (31 ksi). These cells were fabricated from the same lot as the texture etched wafers. As in Figure 5-7 the strength of completed cells appears to be increased by metallization.

5. A twist strength distribution of completed cells (lot A) is also plotted in Figure 5-7. The strength of these completed cells is lower than that of texture etched wafers. No detailed information on the cell process is available. Preliminary examination indicated that chips and flaws were present on the cells of lot A. Figure 5-9 shows an example of cell cracking originating from an edge chip. Quantitative measurements of edge chips and surface flaws and correlation with the strength of cells will be made later. It is likely that chips and flaws are generated from cell processing and handling. A rather small slope and a long tail are seen at the low stress points of the strength distribution curve of cell lot A. Cells
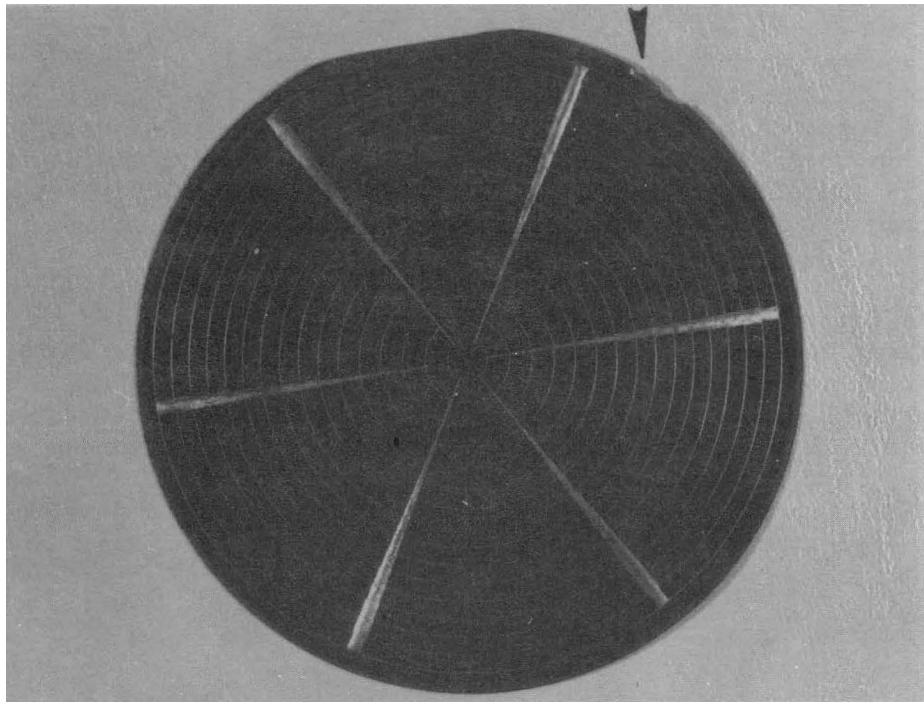
Figure 5-9. Typical Fractured Cell with Edge Chip

which fail at the low stresses of the distribution curve are more
likely to crack during subsequent panel assembly, QA testing, and/or
field service. Proof tests may be used to screen out weak cells prior
to panel assembly.

6.   The comparison of the strength of mesa etched and anti-reflection
(A/R) coated wafers with that of texture etched wafers of the same lot
(lot F) is shown in Figure 5-8. Mesa etching and A/R coating tends to
increase strength slightly at the higher stress levels, suggesting
that mesa etching and A/R coating processes are not effective in
reducing large surface flaws.

7.   The comparison of the strength of pre-ohmic cells and that of
completed cells of the same lot (lot A) is shown in Figure 5-8. The
twist strengths at 50% fracture probability for pre-ohmic cells and
completed cells are approximately 172 MNm^{-2} (25 ksi) and 152 MNm^{-2}
(22 ksi), respectively. Completed cells were processed from pre-ohmic
patterned cells by putting on metallization. The major metallization
processes of this manufacturer include palladium silicide, electroless
nickel plating, and Sn-Pb soldering. The total thickness of this
metallization is approximately 0.1 mm. The strength of completed
metallized cells should be greater than that of pre-ohmic cells. As
seen in Figure 5-8, however, the strength of completed (metallized)
cells was found to be lower than that of pre-ohmic cells at most
stress levels of the strength distribution curves. This observation
is the opposite of the expectation. As previously described, edge

5-9

chips and surface flaws are related to the weakening of the completed cell lot A. These chips and flaws were apparently extended and generated by the metallization process. It should be pointed out that both strength distribution curves of pre-ohmic and completed cells have long tails extending to the low stress levels. Since it appears that the large critical flaws obtained in a cell process step are carried on to the subsequent processes, extension of these flaws under stress is expected. Proof tests should be used to eliminate those wafers and cells of the lower strength at the early stages of processing.

8.   As mentioned in Section IV C, scotch tape was applied on the compressive surface of test specimens undergoing cylindrical bending and biaxial strength tests to retain the segments after fracture. Tape was not used on specimens undergoing the four-point twisting test, since shear stress existed on both surfaces of the test specimen; therefore, those specimens shattered as shown in Figure 5-10. Specimens which fractured into smaller fragments were found to have greater strength than those which fractured into larger fragments.

E.   EFFECT OF LOTS ON THE STRENGTH OF WAFERS AND CELLS

Several lots of texture etched wafers and completed cells were tested to determine the effect of lot numbers on the strength of wafers and cells. The twist strengths of texture etched wafers of several lots are plotted in Figure 5-11. The twist strengths of completed cells of several lots are shown in Figure 5-12. Appreciable strength variations were observed among lots for both texture etched wafers and completed cells. It should be pointed out that Lot E of the texture etched wafers has a long tail in the low strength end of the distribution curve while Lots B and F show very small scatter in strength data, as shown in Figure 5-11. This implies that proper texture etching may be able to increase the strength of silicon wafers. More studies need to be done to elucidate the effect of texture etching on the strength of silicon wafers. However, improved control of process procedures and better handling during processing should reduce the variations in mechanical strength of solar cells among lots.
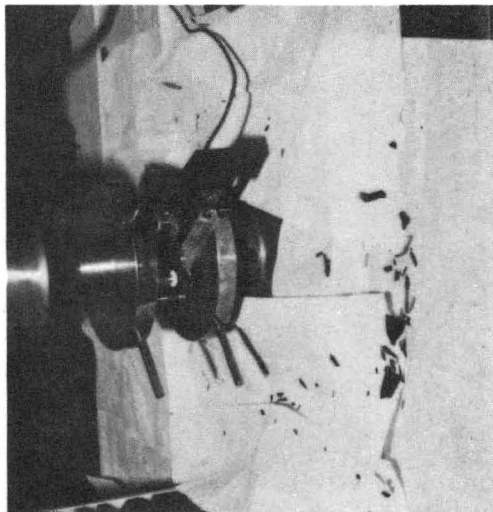
Large Fragments

Small Fragments

Shatter
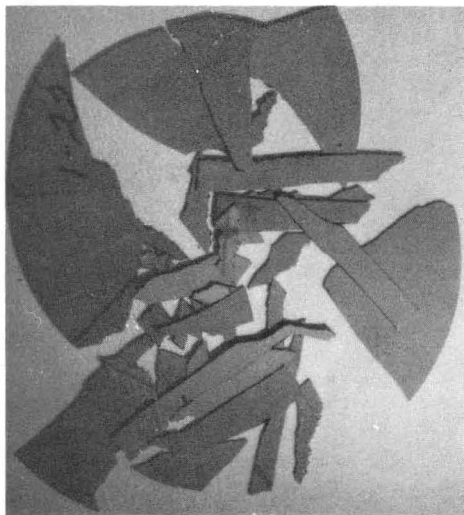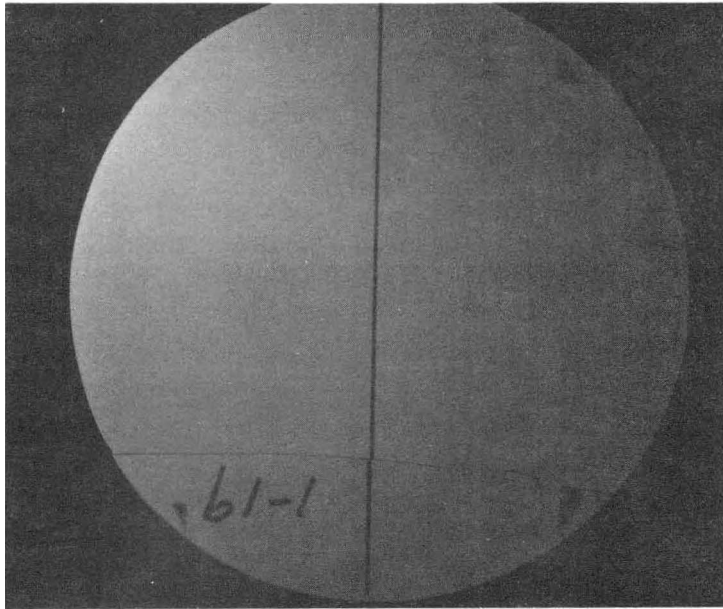
Figure 5-10. Typical Fractures of Silicon Wafers Subjected
to Four-point Twisting
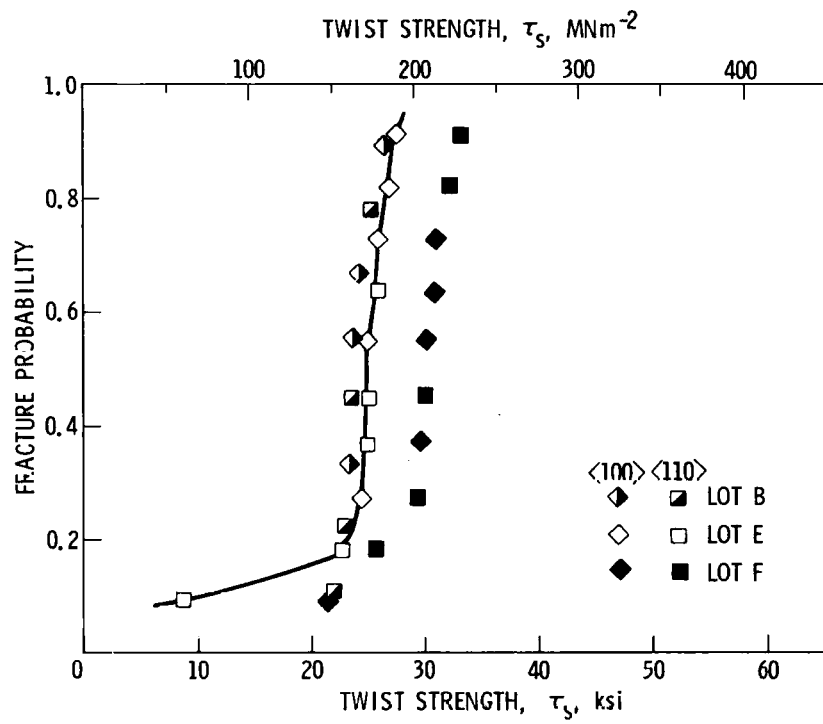
Figure 5-11. Effect of Lots on Twist Strength of Texture Etched Wafers
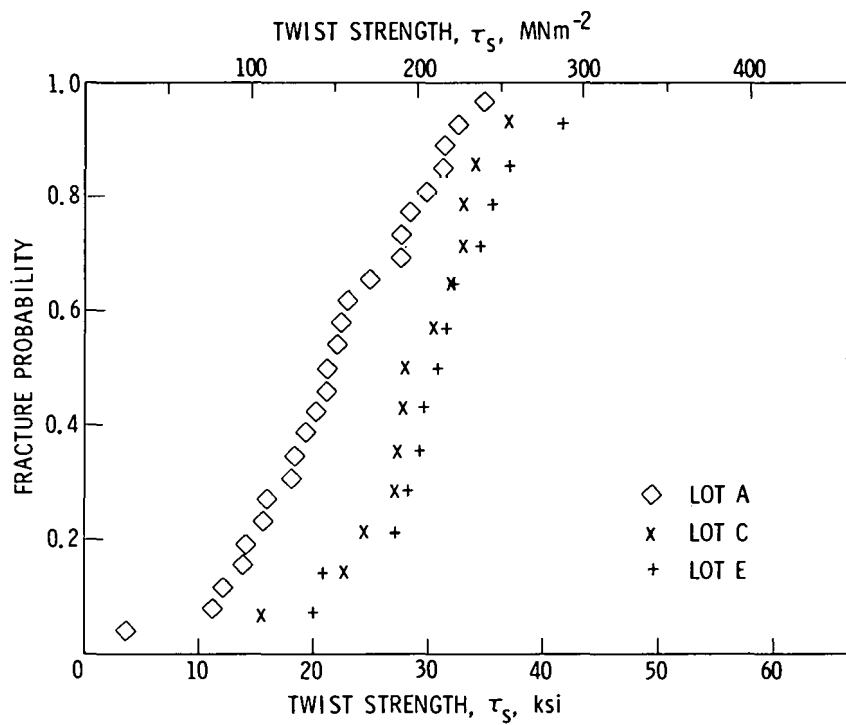
Figure 5-12. Effect of Lots on Twist Strength of Completed Cells

SECTION VI

CONCLUSIONS

The following conclusions have been drawn from the results of
this test program:

1. The four-point twisting test is recommended as a standard test
method for measurement of the mechanical strength of silicon solar
cells because it has the following advantageous characteristics:

    (a)   Simple loading configuration

    (b)   Self-alignment

    (c)   Symmetrical

    (d)   Easy to perform

    (e)   Stresses almost the entire cell specimen, including the
          edge

2. The Weibull distribution plot of strength data is useful to
describe the strength characteristics of each type of wafer or cell at
various cell process steps and to describe the flaw distribution of
each sample type.

3. The effect of crystalline orientation on the strength of silicon
solar cells is small, since the strength of a silicon wafer is
controlled by crack initiation but not crack propagation.

4. Chemical polishing is useful for reducing the surface flaws of
silicon wafers. A greater than twofold increase in mean strength of
wafers results from chemical polishing. However, it is more effective
in the reduction of the smaller flaws than of larger flaws. A greater
increase in strength is found at higher strengths than at the lower
strength portion of the distribution curve.

5. Texture etching reduces somewhat the surface damage resulting
from ingot cutting, so that the overall strength of a textured wafer
is higher than that of an as-cut wafer, although the mean strength of
texture etched wafers is lower than that of chemically polished wafers.

6. Mechanical edge rounding does not produce significant change in
the strength of the silicon wafer.

7. Mesa etching and anti-reflection coating of wafers and pre-ohmic
(patterned) cells result in little change in strength from the prior
process.

8.   The strength of wafers and cells varied from lot to lot. Edge flaws in samples which were generated during processing and handling were found to be the controlling factor in the measured strength of samples in a lot.

9.   A long tail at the low stress portion of the strength distribution curve was found for several types of samples. The wafers or cells in the low strength distribution are likely to be fractured during subsequent cell processing and handling or in the field service. A proof test would be useful to eliminate these samples before the subsequent cracking occurs.

SECTION VII

RECOMMENDATIONS

The information presented in this report is the result of work carried out during the first phase of a continuing effort to evaluate the fracture strength of silicon solar cells. The recommendations that follow are of further work to be carried out during the second phase of this test program to generate additional information important for engineering design use. The recommendations are:

(1) Continue and complete the Weibull statistical analysis of the present strength data on silicon solar cells.

(2) Design and fabricate a four-point twisting test jig adjustable for various sizes (e.g., up to 6-inches in diameter) and shapes (e.g., square, rectangular) of solar cells.

(3) Investigate the four-point twisting method in more detail analytically and experimentally.

(4) Perform further tests of cell physical characteristics on cells from various manufacturers to determine important fracture-controlling factors such as edge and surface conditions resulting from various wafering and processing, as well as the nature of sheet, shape, size, etc.

(5) Conduct failure analysis to determine the nature and source of the flaw controlling the fracture of solar cells.

(6) Establish proof test levels for critical cell processes.

(7) Determine QA procedures and mechanical strength criteria for silicon solar cells.

(8) Evaluate the effect of chemical polishing and texture etching on the strength of silicon wafers.

(9) Evaluate tearing fracture properties of silicon by measuring the critical stress-intensity factor for Mode III crack extension or $K_{III\ C}$.

REFERENCES

1. Anhalt, K. J., "Quality Assurance, Block III: Experience to March 1, 1979," presented at Low-Cost Solar Array Project 12th Project Integration Meeting, California Institute of Technology, Pasadena, CA, April 4-5, 1979.

2. Shumka, A. and K. H. Stern, "Some Failure Modes and Analysis Techniques for Terrestrial Solar Cell Modules," Proceedings of 13th IEEE Photovoltaic Specialists Conference, pp. 824-34, Washington, D.C., June 5-8, 1978.

3. Weibull W., "The Phenomenon of Rupture in Solids," Ingeniors Vetenskaps Akademiens, Handlingar, Vol. 153, pp. 1-55, (1939).

4. Weibull, W., "A Statistical Distribution Function of Wide Applicability," J. Appl. Mech., Vol. 18, pp. 293-297, (1951).

5. ASTM C 158-72, "Standard Methods of Flexure Testing of Glass (Determination of Modulus of Rupture)."

6. Giovan, M. N., "An Experimental and Statistical Study of the Uniaxial and Equibiaxial Strength of a Brittle Material," M. S. Thesis in Engineering, UCLA, 1978.

7. ASTM F394-74T, "Tentative Test Method for Biaxial Flexure Strength (Modulus of Rupture) of Ceramic Substrates."

8. Vitman, F. F., Bartenev, G. M., Pukh, V. P., and L. P. Tsepkov, "A Method for Measuring the Strength of Sheet Glass," Steklo i Keramika, Vol. 19, No. 8, pp. 9-11, August 1962.

9. Wachtman, J. B., Jr., Capps, W. and J. Mandel, "Biaxial Flexure Tests of Ceramic Substrates," J. of Materials, Vol. 7, No. 2, pp. 188-94, (1972).

10. Kirstein, A. F. and R. M. Wooley, "Symmetrical Bending of Thin Circular Elastic Plates on Equally Spaced Point Supports," J. of Research, (National Bureau of Standards), Vol. 71C, No. 1, pp. 1-10, (1967).

11. Peery, D. J., Aircraft Structures, Chapter 13, McGraw-Hill, 1960.

12. Wiederhorn, S. M. and N. J. Tighe, "Proof-testing of Hot-Pressed Silicon Nitride," J. Matl. Science, Vol. 13, pp. 1781-93, (1978).

APPENDIX A

STRESS CALCULATION OF TEST CONFIGURATIONS

1. Cylindrical Bending

The loading condition of a cell under cylindrical bending is shown in Figure 3-1. The fiber stress or modulus of rupture (MOR) can be calculated by

$$\sigma = \frac{3P(L-\ell)}{2 \, d \, t^2} \qquad (A-1)$$

where

P = total applied force

L = outer span

ℓ = center span

t = thickness of the cell specimen

d = width of the beam under stress. In this case, d is the chord length of the cell specimen parallel to the loading line, varying from inner loading line length D' to diameter D, depending upon the location of the fracture originating flaw (as shown in Figure 3-1).

For a 76 mm (3 in.) diameter cell in which ℓ is 25.4 mm (1 in.), D' is calculated to be 71 mm (2.8 in.). The difference between D and D' is small. Therefore, the MOR value of a cell under cylindrical bending can be calculated approximately by

$$\sigma = \frac{3P(L-\ell)}{2 \, D \, t^2} \qquad (A-2)$$

2. Biaxial Flexure Strength

This loading condition is shown in Figure 3-2. The maximum radial and tangential stresses ($\sigma_{r_{max}}$ and $\sigma_{t_{max}}$, respectively) can be calculated (Reference 9) by

$$\sigma_{r_{max}} = \sigma_{t_{max}} = -\frac{3}{4\pi} \frac{P}{t^2} (X - Y) \qquad (A-3)$$

where

$$X = (1 + \nu) \ln \left(\frac{b}{c}\right)^2 + \frac{1 - \nu}{2} \left(\frac{b}{c}\right)^2$$

$$Y = (1 + \nu) \left[1 + \ln \left(\frac{a}{c}\right)^2\right] + (1 - \nu) \left(\frac{a}{c}\right)^2$$

In these equations,

c = radius of the specimen

a = radius of the concentric circle of supporting points

b = radius of the loaded area of the specimen

ν = Poisson's Ratio

3.   Four-Point Twisting

A stress analysis of a rectangular cross-sectional member subjected to a torsion, T, the maximum shear stress, τ_s, can be calculated by an equation (Reference 11) as

$$\tau_s = \frac{T}{\alpha d t^2} \qquad\qquad \text{(A-4)}$$

where

α = a constant which is a function of b/t,

d = width of the specimen

A cell specimen subjected to four-point twisting is shown schematically in Figure 3-3. In this case, the applied torsional moment, T, is given by the expression

$$T = \frac{P}{2} s \qquad\qquad \text{(A-5)}$$

where

P is the total fracture force

s is the distance between the torsional forces.

Since a solar cell is a very thin disc, the ratio $b/t \rightarrow \infty$. Therefore (Reference 11) $\alpha = 1/3$, and it can be approximated that

$$d \approx s$$

A-2

Substituting these values and Equation A-5 into Equation A-4, the twist (shear) stress can be estimated by

$$\tau_s = \frac{3P}{2t^2} \qquad\qquad (A-6)$$

A-3

APPENDIX B

MEASURED CELL STRENGTH DATA

As-cut and chemically polished silicon wafers were used to
evaluate the modulus of rupture (MOR) strength of silicon in several
crystalline orientations using the cylindrical bending test. The
results for as-cut wafers undergoing the cylindrical bending test in
<100> and <110> orientations are given in Tables B-1 and B-2,
respectively. The results for chemically polished wafers undergoing
cylindrical bending in <110> and 22.5° off <110> (direction halfway
between <100> and <110> orientations) are given in Tables B-3 and B-4,
respectively. The test results for as-cut, chemically polished, and
edge rounded wafers are given in Tables B-8, B-9, and B 10,
respectively.

As-cut, chemically polished, and texture etched silicon wafers
were evaluated by their performance in the biaxial flexure strength
test. The results are given in Tables B-5, B-6, and B-7, respectively.

The four-point twisting test was used to evaluate the twist
strength of wafers and cells as a function of cell process steps. The
test results for as-cut, chemically polished, and edge rounded wafers
are given in Tables B-8, B-9, and B-10, respectively. The effect of
lots on the twist strength test results for texture etched wafers is
given in Tables B-11 to B-13. The results for mesa etched and A/R
coated wafers and pre-ohmic cells under four-point twisting are given
in Tables B-14 and B-15, respectively. The twist strength test
results for completed cells of several lot numbers are given in Tables
B-16 to B-18.

Table B-1. Results of As-Cut Wafers Under Cylindrical Bending Tests in <100>

Specimen No.	Fracture Force (lb)	Minimum Thickness (in.)	Center Deflection at Failure (in.)	Fracture Stress (psi)
1-57	8.9	0.0171	0.055	17,745
1-58	8.9	0.0173	0.055	17,337
1-59	8.1	0.0172	0.047	15,962
1-60	9.9	0.0172	0.058	19,510
1-61	10.0	0.0172	0.057	19,707
1-62	10.0	0.0171	0.058	19,938
1-63	9.1	0.0171	0.055	18,143
1-64	8.3	0.0171	0.048	16,548
1-65	10.0	0.0171	0.058	19,938
1-66	--*	0.0172	--	--
1-67	10.3	0.0172	0.059	20,298
1-68	9.9	0.0172	0.059	19,510

*Failed before test.

Table B-2. Results of As-Cut Wafers Under Cylindrical
Bending Tests in <110>

Specimen No.	Fracture Force (lb)	Minimum Thickness (in.)	Center Deflection at Failure (in.) ·	Fracture Stress (psi)
1-44	8.7	0.0173	0.057	16,947
1-45	9.0	0.0175	0.054	17,133
1-46	8.6	0.0174	0.046	16,560
1-47	9.1	0.0173	0.050	17,726
1-48	10.0	0.0174	0.047	19,256
1-49	9.0	0.0174	0.046	17,330
1-50	8.8	0.0173	0.051	17,142
1-51	8.4	0.0173	0.040	16,363
1-52	8.2	0.0171	0.040	16,349
1-53	8.3	0.0172	0.043	16,356
1-54	8.9	0.0172	0.044	17,539
1-55	8.7	0.0172	0.042	17,145
1-56	8.7	0.0172	0.045	17,145

Table B-3. Results of Chemically Polished Wafers Under Cylindrical Bending in <110>

Specimen No.	Fracture Force (1b)	Minimum Thickness (in.)	Center Deflection at Failure (in.)	Fracture Stress (psi)
3-57	10.6	0.0151	0.077	27,103
3-58	18.8	0.0150	0.136	48,713
3-59	15.8	0.0151	0.108	40,399
3-60	17.7	0.0150	0.123	45,863
3-61	13.8	0.0150	0.088	35,757
3-62	15.9	0.0150	0.118	41,199
3-63	12.3	0.0148	0.102	32,738
3-64	16.3	0.0150	0.113	42,235
3-65	17.3	0.0150	0.119	44,826
3-66	15.6	0.0150	0.117	40,421
3-67	15.1	0.0151	0.107	38,609
3-68	9.3	0.0148	0.066	24,753
3-69	7.3	0.0149	0.054	19,170

Table B-4. Results of Chemically Polished Wafers Under Cylindrical Bending in 22.5° <110>

Specimen No.	Fracture Force (lb)	Minimum Thickness (in.)	Center Deflection at Failure (in.)	Fracture Stress (psi)
3-70	9.0	0.0146	0.076	24,615
3-71	15.3	0.0148	0.117	40,723
3-72	20.3	0.0150	>0.137	52,600
3-73	7.6	0.0150	0.062	19,692
3-74	12.7	0.0150	0.108	32,907
3-75	15.7	0.0147	0.128	42,358
3-76	16.2	0.0148	0.129	43,118
3-77	15.5	0.0148	0.125	41,255
3-78	18.1	0.0150	>0.137	46,899
3-79	17.7	0.0150	0.129	45,863
3-80	17.9	0.0149	0.132	47,006
3-81	10.1	0.0149	--*	26,523

*Extensometer malfunction.

Table B-5. Results As-Cut Wafers Under Biaxial Strength Test

Specimen No.	Fracture Force (lb)	Center Thickness (in.)	Center Deflection at Failure (in.)	Fracture Stress (psi)
1-32	7.6	0.0178	--	35,740
1-33	5.2	0.0179	--	24,181
1-34	6.1	0.0178	0.062	28,686
1-35	5.9	0.0179	0.053	27,437
1-36	5.2	0.0178	0.050	24,454
1-37	5.9	0.0178	0.055	27,746
1-38	6.0	0.0177	0.052	28,536
1-39	6.6	0.0178	0.055	31,038
1-40	5.6	0.0178	0.050	26,335
1-41	5.6	0.0175	0.047	27,246
1-42	6.3	0.0177	0.052	29,963
1-43	6.5	0.0176	0.052	31,266

Table B-6.   Results of Chemically Polished Wafers Under
Biaxial Strength Test

Specimen No.	Fracture Force (lb)	Center Thickness (in.)	Center Deflection at Failure (in.)	Fracture Stress (psi)
3-44	4.6	0.0159	0.053	27,111
3-45	8.6	0.0155	0.080	53,336
3-46	19.4	0.0154	0.167	121,884
3-47	11.8	0.0154	0.115	74,136
3-48	9.0	0.0155	0.100	55,817
3-49	6.6	0.0158	0.080	39,393
3-50	8.2	0.0157	0.085	49,568
3-51	11.3	0.0155	0.110	70,081
3-52	16.9	0.0155	0.140	104,812
3-53	12.5	0.0153	0.120	79,563
3-54	11.9	0.0153	0.115	75,744
3-55	14.9	0.0153	0.140	94,840
3-56	13.8	0.0152	0.132	88,998

Table B-7. Results of Texture Etched Wafers (Edge Rounded) Under Biaxial Strength Test

Specimen No.	Fracture Force (lb)	Center Thickness (in.)	Center Deflection at Failure (in.)	Fracture Stress (psi)
5-1	9.8	0.0175	0.080	47,680
5-2	13.2	0.0173	0.098	65,716
5-3	10.4	0.0173	0.080	51,776
5-4	11.0	0.0174	0.085	54,135
5-5	13.4	0.0174	0.100	65,947
5-6	12.9	0.0176	0.098	62,051
5-7	10.0	0.0175	0.080	48,653
5-8	7.4	0.0175	0.068	36,003
5-9	10.1	0.0176	0.078	48,583
5-10	12.1	0.0173	0.090	60,239
5-11	9.5	0.0173	0.075	47,295
5-12	12.4	0.0171	0.095	63,185
5-13	11.1	0.0175	0.088	54,005
5-14	10.8	0.0174	0.085	53,151
5-15	12.3	0.0176	0.090	59,165
5-16	12.4	0.0176	0.093	59,646
4=17	11.6	0.0176	0.088	55,798

Table B-8. Results of As-Cut Wafers Under Four-point Twisting

Specimen No.	Fracture Force (lb)	Minimum Thickness (in.)	Relative* Deflection at Failure (in.)	Fracture Stress τ_s (psi)
1-11	4.5	0.0172	0.095	13,462
1-12	--**	0.0174	--	--
1-13	4.7	0.0172	0.083	14,060
1-14	4.3	0.0171	0.077	13,014
1-15	4.4	0.0169	0.083	13,634
1-16	4.5	0.0172	0.090	13,462
1-17	4.1	0.0176	0.078	11,714
1-18	4.9	0.0170	0.091	15,005
1-19	2.2	0.0170	0.052	6,737
1-20	5.0	0.0171	0.088	15,133
1-21	4.2	0.0171	0.077	12,712

*Relative deflection between two pairs of twisting forces.
**Specimen failed before test.

Table B-9. Results of Chemically Polished Wafers Under
Four-point Twisting

Specimen No.	Fracture Force (lb)	Minimum Thickness (in.)	Relative Deflection at Failure (in.)	Fracture Stress τ_s (psi)
3-10	5.2	0.0142	0.137	22,823
3-11	9.9	0.0142	0.210	43,451
3-12	9.9	0.0145	0.210	41,678
3-13	8.3	0.0144	0.186	35,424
3-14	7.6	0.0147	0.146	31,126
3-15	2.8	0.0145	0.080	11,786
3-16	11.4	0.0147	0.215	46,689
3-17	9.4	0.0145	0.180	39,567
3-18	7.4	0.0145	0.160	31,149
3-19	4.7	0.0146	0.107	19,514
3-20	8.1	0.0145	0.170	34,095
3-21	3.9	0.0147	0.093	15,973
3-22	7.5	0.0145	0.145	31,570
3-23	5.9	0.0147	0.135	24,164
3-24	5.5	0.0145	0.177	23,151
3-25	8.7	0.0147	0.176	35,631
3-26	5.1	0.0143	0.125	22,072
3-27	10.0	0.0148	0.193	40,404
3-28	13.9	0.0147	0.256	56,928
3-29	5.4	0.0142	0.117	23,701
3-30	8.5	0.0147	0.180	34,812
3-31	7.2	0.0145	0.154	30,307

Table B-10. Results of Edge Rounded Wafers Under
Four-point Twisting

Specimen No.	Fracture Force (lb)	Minimum Thickness (in.)	Relative Deflection at Failure (in.)	Fracture Stress τ_s (psi)
2-1	4.7	0.0171	0.125	14,225
2-2	4.9	0.0165	0.113	15,928
2-3	5.0	0.0175	0.100	14,449
2-4	2.8	0.0170	0.065	8,574
2-5	4.9	0.0172	0.105	14,658
2-6	3.8	0.0172	0.092	11,368
2-7	4.5	0.0170	0.100	13,780
2-8	4.1	0.0167	0.095	13,011
2-9	4.1	0.0167	0.093	13,011
2-10	3.5	0.0169	0.075	10,845

Table B-11. Results of Texture-Etched Wafers Lot B Under
Four-point Twisting

Specimen No.	Fracture Force (lb)	Minimum Thickness (in.)	Relative Deflection at Failure (in.)	Fracture Stress τ_s (psi)
5-28	7.5	0.0165	0.100	24,380
5-29	7.4	0.0166	0.103	23,766
5-30	7.7	0.0161	0.110	26,289
5-31	7.2	0.0165	0.100	23,405
5-32	7.1	0.0165	0.115	23,080
5-33	6.8	0.0160	0.110	23,508
5-34	6.8	0.0165	0.110	22,105
5-35	7.5	0.0162	0.120	25,292

Table B-12. Results of Texture-Etched Wafers Lot E Under
Four-point Twisting

Specimen No.	Fracture Force (lb)	Minimum Thickness (in.)	Relative Deflection at Failure (in.)	Fracture Stress τ_s (psi)
5-38	7.8	0.0174	0.130	22,800
5-39	2.8	0.0168	0.063	8,780
5-40	8.9	0.0174	0.125	26,016
5-41	8.1	0.0169	0.127	25,099
5-42	8.0	0.0168	0.125	25,085
5-43	8.7	0.0169	0.150	26,958
5-44	8.5	0.0170	0.140	26,029
5-45	7.5	0.0164	0.145	24,678
5-46	8.3	0.0170	0.145	25,417
5-47	9.0	0.0170	0.143	27,561

Table B-13. Results of Texture-Etched Wafers Lot F Under
Four-point Twisting

Specimen No.	Fraction Force (lb)	Minimum Thickness (in.)	Relative Deflection at Failure (in.)	Fracture Stress τ_s (psi)
5-18	9.8	0.0167	0.135	31,098
5-19	9.5	0.0169	0.141	29,437
5-20	9.9	0.0170	0.135	30,317
5-21	6.6	0.0165	0.110	21,455
5-22	9.7	0.0166	0.135	31,153
5-23	10.6	0.0168	0.140	33,238
5-24	10.3	0.0168	0.155	32,297
5-25	8.6	0.0172	0.115	25,727
5-26	9.7	0.0170	0.140	29,704
5-27	9.4	0.0166	0.160	30,189

Table B-14. Results of Mesa Etch and A/R Coated Wafers Lot F
Under Four-point Twisting

Specimen No.	Fraction Force (lb)	Minimum Thickness (in.)	Relative Deflection at Failure (in.)	Fracture Stress τ_s (psi)
6-1	13.2	0.0166	0.225	42,394
6-2	7.0	0.0169	0.135	21,690
6-3	11.5	0.0168	0.175	36,006
6-4	10.4	0.0170	0.155	31,848
6-5	.8.95	0.0166	0.135	28,744
6-6	8.6	0.0168	0.155	26,966
6-7	10.6	0.0170	0.170	32,460
6-8	10.0	0.0167	0.155	31,733
6-9	5.15	0.0168	0.090	16,149
6-10	11.7	0.0168	0.183	36,687

Table B-15. Results of Pre-Ohmic Cells Lot A Under
Four-point Twisting

Specimen No.	Fracture Force (lb)	Minimum Thickness (in.)	Relative Deflection at Failure (in.)	Fracture Stress τ_s (psi)
7-1	7.9	0.0168	0.125	24,771
7-2	8.2	0.0175	0.115	23,696
7-3	7.5	0.0168	0.118	23,517
7-4	8.2	0.0170	0.120	25,111
7-5	7.5	0.0165	0.133	24,380
7-6	7.5	0.0172	0.125	22,436
7-7	8.1	0.0169	0.137	25,099
7-8	7.1	0.0170	0.115	21,742
7-9	7.9	0.0170	0.113	24,192
7-10	11.6	0.0169	0.150	35,944
7-11	1.5	0.0169	0.040	4,648
7-12	10.3	0.0169	0.150	31,916

Table B-16. Results of Completed Cells Lot A Under Four-point Twisting

Specimen No.	Fracture Force (lb)	Minimum Thickness (in.)	Relative Deflection at Failure (in.)	Fracture Stress τ_s (psi)
C-1	5.1	0.0170	0.090	15,618
C-2	1.2	0.0168	0.035	3,763
C-3	7.5	0.0173	0.135	22,178
C-4	7.3	0.0161*	0.130	24,924
C-5	6.3	0.0166*	0.115	20,233
C-6	4.5	0.0170	0.090	13,780
C-7	4.5	0.0168	0.085	14,110
C-8	3.6	0.0168	0.070	11,288
C-9	8.5	0.0165	0.145	27,631
C-10	10.7	0.0165	0.160	34,782
C-11	8.4	0.0164	0.140	27,640
C-12	9.5	0.0160	0.165	32,842
C-13	8.7	0.0159	0.143	30,456
C-14	9.1	0.0160	0.140	31,459
C-15	9.3	0.0162	0.145	31,361
C-16	8.1	0.0159	0.140	28,355
C-17	5.0	0.0151	0.120	19,407
C-18	6.0	0.0171	0.105	18,159
C-19	5.6	0.0177	0.110	15,819
C-20	6.8	0.0169	0.133	21,071
C-21	7.6	0.0178	0.130	21,228
C-22	4.0	0.0170*	0.086	12,249
C-23	7.3	0.0170	0.0135	22,355
C-24	6.8	0.0180	0.125	18,574
C-25	7.5	0.0170	0.133	22,967

*Large variation in thickness (over 3 mils from maximum point).

B-17

Table B-17. Results of Completed Cells Lot C Under
Four-point Twisting

Specimen No.	Fracture Force (lb)	Minimum Thickness (in.)	Relative Deflection at Failure (in.)	Fracture Stress τ_s (psi)
CR-1	9.4	0.0175	0.123	27,164
CR-2	8.6	0.0177	0.120	24,294
CR-3	11.4	0.0175	0.145	32,944
CR-4	9.5	0.0174	0.130	27,770
CR-5	10.0	0.0170	0.135	30,623
CR-6	9.2	0.0170	0.135	28,173
CR-7	12.6	0.0173	0.157	37,258
CR-8	11.5	0.0173	0.167	34,005
CR-9	11.3	0.0174	0.175	33,031
CR-10	8.9	0.0170	0.140	27,254
CR-11	10.2	0.0168	0.155	31,983
CR-12	7.7	0.0173	0.125	22,769
CR-13	5.5	0.0177	0.065	15,537

Table B-18. Results of Completed Cells Lot E Under
Four-point Twisting

Specimen No.	Fracture Force (lb)	Minimum Thickness (in.)	Relative Deflection at Failure (in.)	Fracture Stress τ_s (psi)
CR-14	9.5	0.0172	0.115	28,419
CR-15	10.2	0.0171	0.125	30,871
CR-16	10.5	0.0178	0.123	29,329
CR-17	12.2	0.0174	0.145	35,662
CR-18	11.0	0.0174	0.123	32,154
CR-19	10.7	0.0173	0.135	31,640
CR-20	10.9	0.0167	0.137	34,589
CR-21	--*	--	--	--
CR-22	--*	--	--	--
CR-23	7.3	0.0176	0.103	20,856
CR-24	9.0	0.0171	0.125	27,239
CR-25	12.1	0.0170	0.178	37,054
CR-26	7.3	0.0180	0.125	19,940
CR-27	10.5	0.0177	0.145	29,661
CR-28	14.8	0.0177	0.195	41,808

*Sample failed before test.